

Analyst

Accepted Manuscript



This is an *Accepted Manuscript*, which has been through the Royal Society of Chemistry peer review process and has been accepted for publication.

Accepted Manuscripts are published online shortly after acceptance, before technical editing, formatting and proof reading. Using this free service, authors can make their results available to the community, in citable form, before we publish the edited article. We will replace this *Accepted Manuscript* with the edited and formatted *Advance Article* as soon as it is available.

You can find more information about *Accepted Manuscripts* in the [Information for Authors](#).

Please note that technical editing may introduce minor changes to the text and/or graphics, which may alter content. The journal's standard [Terms & Conditions](#) and the [Ethical guidelines](#) still apply. In no event shall the Royal Society of Chemistry be held responsible for any errors or omissions in this *Accepted Manuscript* or any consequences arising from the use of any information it contains.



Journal Name

ARTICLE

Sensing applications of luminescent carbon based dots

Yongqiang Dong¹, Jianhua Cai¹, Xu You and Yuwu Chi*Received 00th January 20xx,
Accepted 00th January 20xx

DOI: 10.1039/x0xx00000x

www.rsc.org/

Carbon based dots (CDs) including carbon quantum dots and graphene quantum dots exhibit unique luminescent properties, such as photoluminescence (PL), chemiluminescence (CL) and electrochemiluminescence (ECL). This review summarizes the sensing application of the CDs taking advantage of their luminescent properties. The working principle, merits, and perspective of CDs based sensors are presented.

1. Introduction

Carbon nanoparticles of less than 10 nm in particle size (usually called carbon dots, carbon quantum dots, or CQDs) and graphene nanosheets of less than 100 nm in lateral size (usually called graphene quantum dots, or GQDs) serving as emerging luminescent carbon nanomaterials have attracted increasing attention.^{1,2} CQDs and GQDs are usually considered as two different kinds of carbon nanomaterials due to different morphology. CQDs were thought to be spherical particles while GQDs were regarded to be layered sheets. Up to now, many reviews have been available for CQDs or GQDs separately.³⁻¹⁴ However, in this review, we merge CQDs and GQDs into carbon-based dots (CDs) based on following considerations. First, both CQDs and GQDs are composed of sp² carbon structures and similar surface functional groups, such as –COOH and –OH groups, and thus they usually exhibit similar luminescent properties, for examples, photoluminescence (PL), chemiluminescence (CL) and electrochemiluminescence (ECL).^{6, 7, 11, 14-17} Second, it is difficult to conclude that CQDs are really spherical in morphology since no height data for CQDs has been provided in most publications on CQDs.¹⁵⁻²⁰ Third, GQDs are not only single-layered, but also multi-layered. The heights of multi-layer GQDs may be close to their lateral sizes.

CDs are usually considered as a class of zero-dimensional nanomaterials, which exhibit unique optical properties due to the quantum confinement and edge effects. Compared to traditional semiconductor based quantum dots (QDs), CDs harbour not only advantages over organic dyes in photostability against photobleaching and blinking, but also lower toxicity and better biocompatibility.^{5,6} Therefore, CDs have attracted significant attention from researchers. Up to now, CDs have been applied in many fields such as sensing, bio-imaging, photovoltaic devices and

catalysis.^{9, 10, 17, 18} In this review, we only focus on CDs-based PL, ECL and CL sensors. We hope this review might be helpful for understanding luminescent properties of CDs and related advances in sensing applications.

2. PL sensors

PL is one of the most important properties of CDs. Although the exact mechanism is still controversial, the PL of CDs is usually attributed to intrinsic state emission, or defect state (or surface state) emission, or even the combination of them. The intrinsic state emission means the radiative recombination of electron-hole pairs in the small sp² clusters that isolated within the sp³ C-O matrix.^{21, 22} The defect state emission refers to the radiative recombination of the excitons (i.e. holes and electrons) from the unpassivated defects on CD surfaces.²³⁻²⁷ The PL properties of CDs could be affected by the surface states,^{1, 24, 25} the oxidation degree,^{28, 29} and the doping of heteroatoms.³⁰⁻³² Advances in synthesis of colourful (ranging from the deep ultraviolet to near-infrared) and high PL quantum yield (PLQY) CDs based on deeper understanding of PL mechanism,^{10, 30, 32} enable extensive PL-based sensing applications of CDs.

2.1 PL sensors based on the interactions between pristine CDs and metal ions

It has been well reported that PL of many CDs can be quenched by some metal ions. In general, the quenching effects result from the coordination reactions between metal ions and the inherent or functionalized groups on the surfaces of CDs. Pristine CDs (i.e. CDs without special functionalization) usually have large quantities of inherent groups such as carboxyl and hydroxyl groups on their surfaces, whereas specially functionalized CDs can have other desired groups. CDs with different surface groups may respond to different metal ions. In this section, various PL quenching mechanisms of CDs by metal ions will be presented in detail.

2.1.1 Aggregation quenching mechanism

The quenching effects of metal ions on the PL of CDs were first reported by Liu et al.³³ They synthesized CDs by hydrothermally treating candle soot in NaOH solution at 200 °C for 12 h, followed by a serial of purification procedures. The yellow PL emission of the

MOE Key Laboratory of Analysis and Detection Technology for Food Safety, Fujian Provincial Key Laboratory of Analysis and Detection Technology for Food Safety, and Department of Chemistry, Fuzhou University, Fujian 350108, China. Corresponding author. Tel./fax: +86 591 22866137.

E-mail address: y.w.chi@fzu.edu.cn (Y. Chi).

¹ These authors contributed equally to this work.

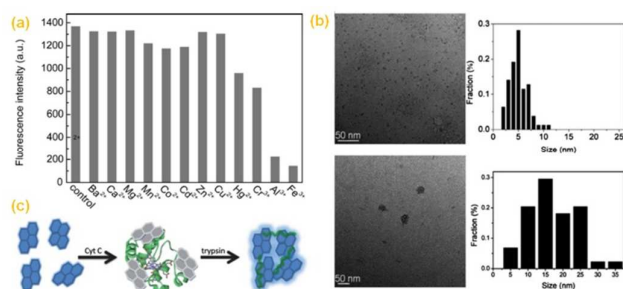


Figure 1. (a) Effect of metal ions on CDs PL intensity. All concentrations of metal ions are 5.0×10^{-6} .³³ (b) TEM images of the CDs (upper) and their self-assembled aggregates by Cyt c (lower). (c) Schematic illustration of the PL biosensor for trypsin based on self-assembled CDs.³⁵ Reproduced by permission from ref. 33; copyright 2011, Springer and ref. 35; copyright 2013, Royal Chemical Society.

obtained CDs could be quenched by many metal ions including Mn^{2+} , Co^{2+} , Hg^{2+} , Cr^{3+} , Al^{3+} , and especially Fe^{3+} (Figure 1a). They ascribed the quenching effect to the aggregation of CDs that was induced by the combination of the inherent massive hydroxyl groups of CDs with those metal ions, and the different quenching abilities of the metal ions to the differences in K_{sp} value of metal hydroxides (the K_{sp} values of $Hg(OH)_2$, $Cr(OH)_3$, $Al(OH)_3$ and $Fe(OH)_3$ are 3.6×10^{-26} , 6.3×10^{-31} , 1.3×10^{-33} , 4.0×10^{-38} , respectively).

Yang et al. synthesized CDs by hydrothermal treating honey.³⁴ They also observed an obvious quenching effect of Fe^{3+} on the PL of the obtained CDs, and further confirmed the aggregation induced quenching by high resolution transmission electron microscopy (HRTEM). In another work, cytochrome c (Cyt c), a protein rich with Fe^{3+} , was also found to be able to quench the PL of CDs. The HRTEM images (Figure 1b) proved the self-assembled aggregation mechanism (Figure 1c).³⁵ Guo et al. used sodium citrate and NH_4HCO_3 for hydrothermally synthesizing a kind of CDs, the PL signal of which could be selectively quenched by Hg^{2+} .³⁶ The quenching effect was attributed to the fact that the interactions between metal ions and the carboxylate or hydroxyl groups made CDs close to each other, which accelerated the non-radiative recombination of the excitons through an effective electron transfer process.

2.1.2 Electron/energy transfer quenching mechanism

However, not all of the PL quenching effects of metal ions resulted

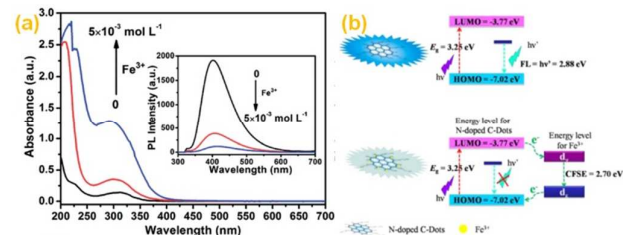


Figure 2. (a) The UV-Vis spectra of the N-CDs mixed with different concentrations of Fe^{3+} in H_2O ($0-5 \times 10^{-3} \text{ mol L}^{-1}$), the inset is the corresponding PL spectra ($\lambda_{exc} = 320 \text{ nm}$).³⁹ (b) Sensing principle of the N-CDs based probe for Fe^{3+} .⁴¹ Reproduced by permission from ref. 39; copyright 2012, Royal Chemical Society and ref. 41; copyright 2014, American Chemical Society.

from the simple aggregation of CDs. Some research groups gave other explanations. Krysmann et al. found that the bright PL emission of CDs synthesized by hydrothermally treating the mixture of citric acid (CA) and ethanolamine could be reduced obviously by Cr^{3+} and Co^{2+} ions instead of Fe^{3+} ion.³⁷ They considered that the PL quenching was related to the selective metal-fluorophore complexation. Similar CDs synthesized by Zhu et al. from the mixture of CA and ethylenediamine also exhibited PL quenching activities toward Fe^{2+} , Zn^{2+} , Cu^{2+} , Co^{2+} , Pb^{2+} , Hg^{2+} , and particularly Fe^{3+} .³⁸ The authors further explained the “metal-fluorophore complexation” in quenching PL of CDs. It was proposed that Fe^{3+} quenched the PL of CDs due to the specific coordination interaction between Fe^{3+} ions and the phenolic hydroxyl groups of the CDs. Teng et al. synthesized a kind of nitrogen-doped CDs (N-CDs) by pyrolyzing konjac flour under an air atmosphere at $470 \text{ }^\circ\text{C}$ for 1.5 h followed by a serial of purification and surface-passivation.³⁹ The PL of the obtained N-CDs could also be sensitively quenched by Fe^{3+} , although the quenching effect would be interfered by Co^{2+} , Ni^{2+} , Zn^{2+} , Ag^+ and Cu^{2+} . It was found that Fe^{3+} could enhance obviously the absorbance of the CDs (Figure 2a), which could be attributed to the combination of Fe^{3+} with N-CDs to form a complex of N-CDs/ Fe^{3+} . Accordingly, an electron transfer mechanism was proposed for the quenching effect of Fe^{3+} on the PL signal of the N-CDs. The quenched PL signal by Fe^{3+} could be recovered by NaOH, L-Arg, or L-Lys, further confirming the electron transfer PL quenching mechanism. Zhao et al. used two different ionic liquids, namely [BMIM][Br] and [BMIM][BF₄] (BMIM refers to 1-butyl-3-methylimidazolium), to synthesize another two kinds of N-CDs, whose PL emissions could be sensitively quenched by Cu^{2+} and Fe^{3+} , respectively.⁴⁰ They attributed the PL quenching by Cu^{2+} or Fe^{3+} to electron or energy transfer. Zhang et al. synthesized N-CDs by hydrothermally treating the mixture of PEG-diamine and CA.⁴¹ Similarly, Fe^{3+} could quench sensitively the PL signal of the obtained N-CDs, while some other metal ions could also quench slightly the PL signal. The authors calculated the highest occupied molecular orbital (HOMO) and lowest unoccupied molecular orbital (LUMO) energy levels of N-CDs and proposed a detailed nonradiative electron-transfer mechanism to explain the PL response of N-CDs to Fe^{3+} (Figure 2b). In brief, the complexation between Fe^{3+} and phenolic hydroxyl groups of N-CDs lead to the splitting of d orbital of Fe^{3+} . Accordingly, electrons in the excited state of N-CDs could be partially transferred to the d orbital of Fe^{3+} , resulting in the PL quenching.

Apparently, the electron or energy transfer mechanisms mentioned above were based on the formation of a “metal-fluorophore complexation”, mainly through the reactions between metal ions and phenolic hydroxyl groups of CDs. However, the complexation may also occur even though the CDs have no hydroxyl groups. For example, Qian et al. synthesized N-CDs through a solvothermal reaction with CCl_4 as the carbon source and diamines as the nitrogen precursor.⁴² The PL signal could also be selectively quenched by Fe^{3+} . The PL quenching was considered to be caused by the excited-state electron transfer due to the formation of CD- Fe^{3+} complexes. It was proposed that the complexation occurred between nitrogen atoms in N-CDs and Fe^{3+} in the absence of carboxyl and hydroxyl groups in N-CDs. The deduction was made by the fact that the quenched PL signal could be recovered by H_3PO_4 ,

which can coordinate with Fe^{3+} to form stable complexes and thus remove Fe^{3+} from the nitrogen sites in N-CDs.

The electron transfer mechanism has also been adopted to explain the quenching effect of other metal ions on the PL of CDs. For example, Ran et al. proposed that Ag^+ could be attached on the surface of CDs via electrostatic interaction, and then reduced to silver nanoparticles (AgNPs).⁴³ The formation of AgNPs/CDs hybrids led to the PL quenching of CDs due to the electron transfer processes. Biothiols was found to be able to reduce Ag^+ and bridge adjoining ANPs with one another. As a result, the PL emission of CDs was quenched completely. Liu et al. found that the PL of CDs from hydroxide-assisted reflux of poly(ethylene glycol) (PEG) could be selectively quenched by Hg^{2+} due to the facilitation of non-radiative electron/hole recombination annihilation through an effective electron transfer process.⁴⁴ The mechanism was further proved by the fact that the lifetime of CDs decreased from 6.0 to 1.0 ns as Hg^{2+} was added into the CD solution. Some other research groups also observed similar phenomenon and proposed similar mechanisms.^{45,46}

In conclusion, the electron transfer mechanisms mentioned above usually involve the formation of metal/CDs complexations and the electron transfer from excited CDs to the metal ions. Usually, the formation of metal/CDs complexes are believed to be related to the functional groups of CDs, such as carboxyl, hydroxyl groups and the doped nitrogen atoms. CDs prepared by different methods may have different functional groups, and thus bind different metal ions. Furthermore, different metal ions may harbour different electron-withdrawing abilities. As a result, the PL signal of different CDs could be selectively quenched by different metal ions. The electron transfer mechanisms have been popular to explain the quenching effect of metal ions on the PL of CDs.

Qu and coworkers provided another electron transfer model for the quenching effect of metal ions on the PL of CDs.⁴⁷ They synthesized CDs from dopamine (DA) by hydrothermal treatment. Many metal ions (Ag^+ , Fe^{2+} , Hg^{2+} and Pb^{2+}) could quench the PL of the obtained CDs, while Fe^{3+} showed the most sensitive quenching. It was proposed that the hydroquinone groups on the surfaces of CDs could be oxidized to quinone species by Fe^{3+} , which could result in the quenching of the PL of CDs due to electron transfer. For the other quenching metal ions, the minor PL decreases resulted from the metal-catechol complexation or metal-quenching effect.

2.1.3 Dynamic quenching mechanism

As mentioned above, Yang et al. observed the quenching behavior of Fe^{3+} on the PL of CDs, and attributed the quenching effect to the formation of "metal-fluorophore complexation".³⁸ However, in one of their follow-up works, another dynamic mechanism was proposed for the PL quenching behaviors of Fe^{3+} .⁴⁸ Four evidences indicated that Fe^{3+} quenched the PL of CDs through a dynamic mechanism. Firstly, the PL quenching fitted well the Stern-Volmer equation. Secondly, the absorbance intensity showed the same linear correlation with the concentration of Fe^{3+} with and without CDs, proving that there was no obvious static intermediate between Fe^{3+} and the CDs. Thirdly, the quenching constant increased when the temperature increased. Fourthly, the addition of Fe^{3+} decreased the lifetime of the CDs.

2.1.4 Enhancing mechanism based on decreasing the dynamic collision between CDs.

Qian et al. found that Ag^+ could enhance the PL of their obtained N-CDs.⁴² It was proposed that Ag^+ could be bonded to N-CDs due to the strong affinity to nitrogen atoms and Ag^+ , positively charging the N-CDs. The positive charges effectively decreased the dynamic collision between N-CDs, leading to the PL enhancement.

The effect of metal ions on the PL of CDs without special functionalization may be a synergistic result of many factors. The exact mechanisms still require further investigations. However, many sensors, both with "signal-off" and "signal-on" models, have been proposed based on the quenching effect of metal ions on the PL of CDs.

2.1.5 Relevant sensing applications

In 2011, Liu et al. reported that their obtained hydroxyls-coated CDs had potential applications in biocompatible nanosensors for measuring Cr^{3+} , Al^{3+} and Fe^{3+} in human body fluids.³³ For example, to detect Cr^{3+} , fluorine ions could be used to mask Al^{3+} , Fe^{3+} . The other two metal ions could be detected in similar ways. Under the optimum conditions, the CDs PL intensity was quenched by Cr^{3+} with a linear range from 1 to 25 μM and a detection limit of 60 nM.

Up to date, many CDs have been used directly as PL probes for "signal-off" sensing of metal ions, especially Fe^{3+} ion.^{34, 40, 41, 48, 49} Also many "signal-off" sensors have been developed for the measurement of Hg^{2+} using CDs directly.^{36, 44-46, 50-53} Most of the sensing systems showed good sensitivities and selectivities, and were applicable in real sample detections. For example, Yang et al. adopted their developed sensor to detect Fe^{3+} in human blood samples.³⁴ Zhang et al. applied their obtained CDs in sensing Fe^{3+} in Hela cells (Figure 3).⁴¹ Yan et al. adopted their obtained CDs for intracellular sensing and imaging of Hg^{2+} , and visual identification of Hg^{2+} in river and mineral water samples.⁵⁰

Ran and coworkers demonstrated that their obtained CDs could be used in the rapid and label-free detection of Ag^+ and biothiols.⁴³ The PL sensors showed good sensitivities for both Ag^+ and biothiols. The

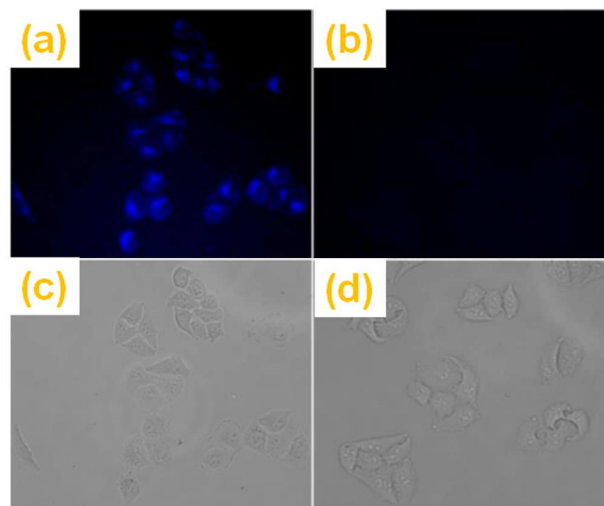


Figure 3. PL microscopy images (a, b) and their corresponding bright-field transmission images (c, d) of Hela cells: (a, c) incubated with $0.4 \text{ mg}\cdot\text{mL}^{-1}$ N-CDs for 6 h at 37°C . (b, d) first incubated with $0.4 \text{ mg}\cdot\text{mL}^{-1}$ N-CDs for 6 h and then incubated with $100 \mu\text{M}$ FeCl_3 for 1 h at 37°C . Reproduced by permission from ref. 41; copyright 2014, American Chemical Society.

detection limit for Ag^+ was 3.5 nM, while those of cysteine (Cys), homocysteine (Hcy) and glutathione (GSH) were 6.2, 4.5 and 4.1 nM, respectively. Wei et al. found that the PL of CDs synthesized from the hydrothermal treatment of corn flour could be selectively quenched by Cu^{2+} .⁵⁴ Accordingly, a PL sensor was constructed for the detection of Cu^{2+} with a calculated detection limit of 1 nM.

Furthermore, some “signal-on” sensors have also been developed. In 2011, Zhao et al. used the CDs prepared from the mixture of CA and $\text{H}_2\text{N}(\text{CH}_2)_{10}\text{COOH}$ by hydrothermal treatment as the PL probes to develop a selective sensor for the detection of phosphate (Figure 4a).⁵⁵ First, the PL signal of CDs was quenched with Eu^{3+} , which was considered to be able to coordinate with the carboxylate groups on the CDs surface and make the CDs aggregated, similar with those mentioned in their another work.³³ Subsequently, the quenched PL signal was recovered with phosphate by removing Eu^{3+} from the surfaces of CDs due to the strong coordination between phosphate and Eu^{3+} (Figure 4b). The sensor showed good performance with a linear response range from 4.0×10^{-7} to 1.5×10^{-5} mol L^{-1} and a detection limit of 5.1×10^{-8} mol L^{-1} , and was successfully applied in detecting phosphate in complicated matrix such as artificial wetlands system. A similar work was also carried out by Bai et al. using a kind of different CDs (synthesized from GO sheets by a hydrothermal method).⁵⁶ Liu and coworkers quenched the PL of CDs with Fe^{3+} instead of Eu^{3+} , and recovered the quenched PL signal with adenosine triphosphate (ATP) rather than phosphate.⁵⁷ Accordingly, a PL sensor was developed for the detection of ATP, with a linear response range of 25–250 μM and a detection limit of 22 μM . Furthermore, the sensor was successfully applied in real samples such as cell lysates and human blood serum. Xu et al. found that the PL signal of CDs quenched by Fe^{3+} could be also recovered

by phosphate.⁵⁸ Therefore, they also developed a “signal-on” sensor for phosphate. Li and co-workers applied their obtained CDs as PL probes for the detection of trypsin, which could cleave peptide bonds of Cyt c into lysine and arginine residues.³⁵ As a result, the PL signal of CDs quenched by Cyt c was recovered. The developed nanosensor showed high selectivity and sensitivity (with a detection limit of 33 ng mL^{-1}).

Qu et al. used the CDs from DA by hydrothermal treatment as the PL probe of DA.⁴⁸ The PL signal was first quenched by Fe^{3+} as has been mentioned above, then was recovered by DA through a competition mechanism. The enhanced PL intensity was proportional to the DA concentration in the range from 0.1 to 10 μM , and the detection limit for DA was 68 nm.

Zhang et al. fabricated a sensor for oxalate based on that the yellow PL emission of CDs from chemical oxidation of activated carbon could be quenched by Cu^{2+} and the quenched PL could be recovered by oxalate.⁵⁹ It was proposed that oxalate could coordinate to Cu^{2+} and thus remove Cu^{2+} from the surfaces of CDs due to competitive interaction with Cu^{2+} between oxalate molecules and CDs. The recovered PL intensity exhibited a linear relationship with the concentration of oxalate in the range of 1.0×10^{-5} to 7.0×10^{-5} mol L^{-1} , and the detection limit for oxalate was 1.0×10^{-6} mol L^{-1} .

2.2 PL sensors based on the interactions between CDs and protons

The PL emissions of some CDs were nearly independent on the pH value of solution.^{60–63} However, most CDs exhibited pH-dependent PL activities. For example, Pan and coworkers found that the CDs synthesized from hydrothermal treatment of GO could emit strong PL in alkaline solutions, while the PL intensity decreased greatly in acidic solutions.^{64–66} Furthermore, the pH effect on the PL intensity of the CDs was reversible (Figure 5a). The authors attributed the PL of their obtained CDs to the free zigzag sites with a carbene-like triplet ground, and accordingly proposed a structural model to explain pH-dependent PL (Figure 5b). In brief, under alkaline conditions, the zigzag sites in the CDs were free and PL-active. However, under acidic solutions, the zigzag sites in the CDs were protonated and PL-inactive. Other researchers also noticed similar pH-dependent PL from their obtained CDs.^{67–69} Many other CDs exhibited quite different responses to the change of pH value (Figure 5c, d).^{32, 36, 37, 41, 42, 70–77} The PL intensities of the CDs were relatively strong in neutral solutions, whereas the PL intensities decreased in strong acidic or/and strong alkaline solutions. Apparently, CDs synthesized by different methods may have different responses to solution pH. It is difficult to propose an exact and general mechanism for the pH effect on the PL of CDs due to the fact that the PL mechanisms of CDs are still open questions. However, people usually considered that the pH effect on the PL of CDs was related to their surface states.

Up to date, some pH sensors have been developed based on the PL of CDs. For example, Zhao et al. found that the PL intensity of CDs obtained by electrochemically oxidizing graphite decreased linearly as the pH was increased gradually over the range from 7 to 14, and proposed that the CDs could be used to monitor reactions that may lead to a minor change in pH.⁷³ Qian et al. reported that the N-CDs synthesized by solvothermal reaction of CCl_4 and 1,2-ethylenediamine could also be used in pH sensor due to the fact

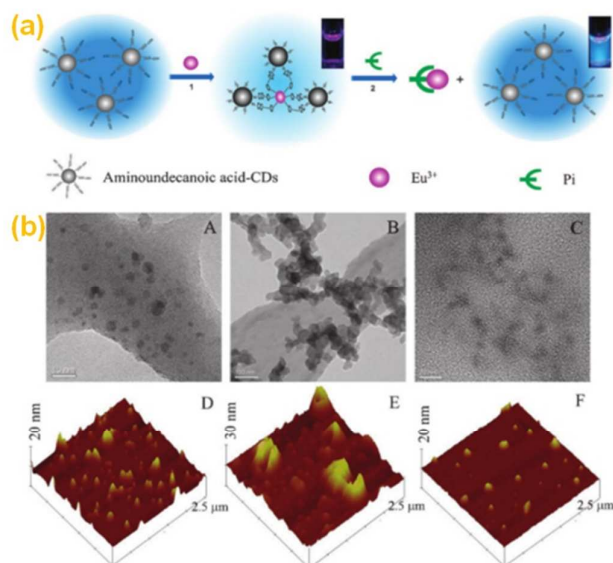


Figure 4. (a) Schematic representation of Pi detection based on the off-on PL probe of CDs adjusted by Eu^{3+} . (b) HRTEM and AFM images of off-on process. CDs alone (scale bar, 10 nm) (A); CDs- Eu^{3+} aggregation (scale bar, 100 nm) (B); CDs- Eu^{3+} aggregation in the presence of Pi (scale bar, 20 nm) (C); CDs alone (D); CDs- Eu^{3+} aggregation (E); CDs- Eu^{3+} aggregation in the presence of Pi on mica (F). Reproduced by permission from ref. 55, copyright 2011, Royal Chemical Society.

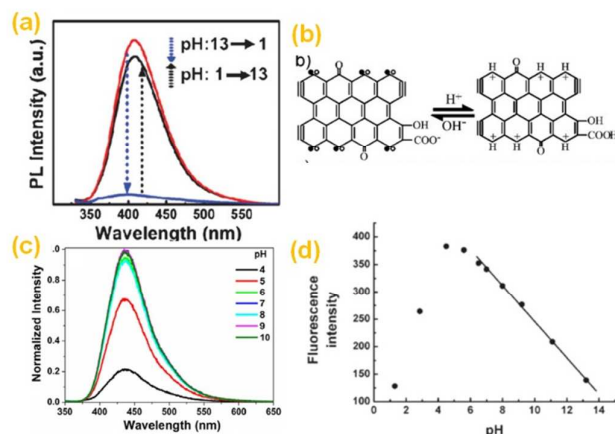


Figure 5. (a), (c) and (d) show effect of the solution pH on the PL intensity of the CDs from hydrothermal treatment of GO,⁶⁴ hydrothermal treatment of sodium citrate in NH_4CO_3 solution,³⁶ and electrochemical oxidation of graphite.⁷³ (b) Models of the CDs in acidic (right) and alkali (left) media. The two models can be converted reversibly depending on pH. The pairing of σ (*) and π (o) localized electrons at carbene-like zigzag sites and the presence of triple bonds at the carbyne-like armchair sites are represented.⁶⁴ Reproduced by permission from ref. 36, copyright 2013, Elsevier; ref. 64, copyright 2010, Wiley-VCH and ref. 73, copyright 2008, Royal Chemical Society.

that the PL intensity was inversely proportional to pH values from 5.0 to 13.5.⁴² Pedro et al. developed a pH sensor using the CDs obtained by the thermal decomposition of ascorbic acid in dimethyl sulfoxide, the PL intensity of which decreased linearly as the pH value varying from pH 4.5 to 11.5.⁷⁸ Nie et al. modified the CDs synthesized by refluxing CHCl_3 and diethylaniline with a pH-sensitive dye, fluorescein isothiocyanate (FITC), to be used as a pH probe.⁷⁹ The FITC-modified CDs exhibited a strong emission peak at 524 nm from FITC, and two peak emissions at 470 and 565 nm from the CDs when excited respectively by 405 and 534 nm light beams. The emission intensity at 524 nm increased with the increase of pH value, while those at 470 and 565 nm decreased gradually. Therefore, two independent standard curves were obtained. It was found that the ratios of PL intensities increased linearly in the range from pH 5 to 8.

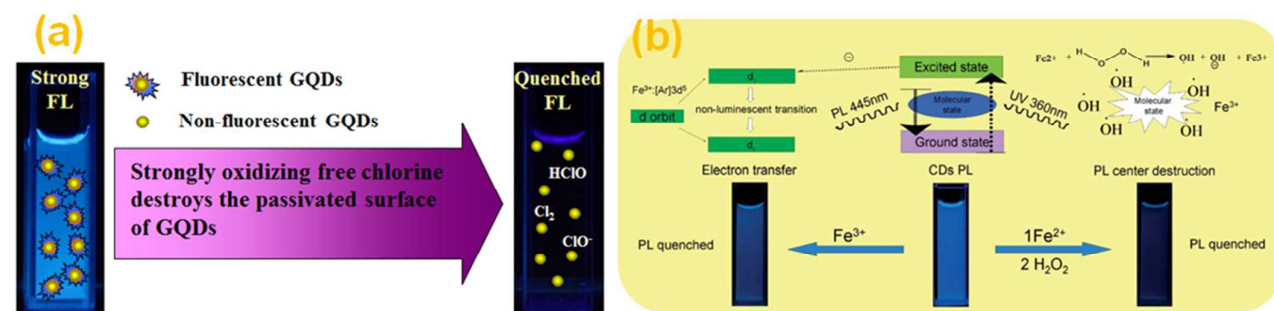


Figure 6. (a) Schematic representation of free chlorine detection based on CDs. The surface passivation was destroyed.⁸¹ (b) Fe^{3+} and H_2O_2 sensors based on visual PL detection. The PL center was destroyed by the formed OH^\bullet free radical.⁴⁷ Reproduced by permission from ref. 47, copyright 2014, Royal Chemical Society and ref. 81, copyright 2012, American Chemical Society.

2.3 PL sensors based on the interactions between pristine CDs and strong oxidants

Free chlorine, a kind of strong oxidizing agent extensively used in water treatment, was found by Chi and coworkers to be able to quench greatly the bright blue PL emission of the CDs synthesized by pyrolysis of CA.^{80, 81} It was proposed that the strong oxidants might destroy the surface passivation of the CDs, leading to the quenching of PL (Figure 6a). Accordingly, a green sensing system has been developed for the sensitive and selective detection of free chlorine in water. The performances of sensing system (linear response from 0.05 to 10 μM with a detection limit of 0.05 μM) were much better than those of the most widely used N-N-diethyl-p-phenylenediamine (DPD) colorimetric method. Finally, the applicability of the proposed sensing system was further confirmed by the successful detection of free residual chlorine in local tap water samples. Some other CDs have also been applied in the sensing of free chlorine, through the same PL quenching mechanism.⁸²

Fenton reagent ($\text{Fe}^{2+}/\text{H}_2\text{O}_2$), a strong oxidant that has been widely used for removing organic molecules, was also found to be able to quench the PL of CDs effectively. The quenching effect of Fenton reagent on PL of CDs was first noticed by Chi and coworkers.⁸¹ Unfortunately, they didn't make any further investigation. The phenomenon was also observed by Qian and coworkers.⁴² However, they attributed the quenching effect to the formation of Fe^{3+} , which was also able to quench the PL of CDs. Yang et al. investigated in detail the quenching mechanism (Figure 6b).⁴⁷ It was proposed that the formation of OH^\bullet free radical, with ultrahigh oxidation potential could destroy the chemical structure of CDs, resulting in the PL center destruction and PL quenching. Accordingly, a sensitive H_2O_2 sensor has been developed, with a low detection limit of 0.9 ppb.

2.4 PL sensors based on the interactions between amino group functionalized CDs and copper ions

To further extend the applications of CDs in sensing, more and more attention has been paid to the functionalization of CDs. Dong et al. used branched polyethylenimine (BPEI) and CA to synthesize highly PL active (with the PL quantum yield, PLQY of 42.5%) BPEI-CDs by thermal treatment.⁸³ The amino groups of BPEI-CDs could

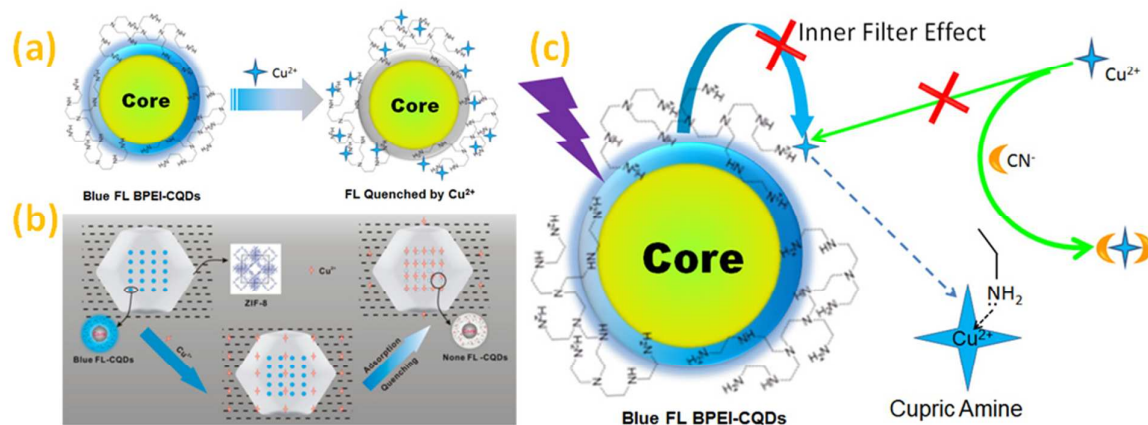


Figure 7. (a) Schematic illustration for sensing of Cu^{2+} based on BPEI-CDs.⁸⁴ (b) Concept and Process for Sensing Cu^{2+} Based on BPEI-CDs encapsulated MOFs.⁸⁹ (c) Diagram for the "recovery" effect of cyanide on the PL of BPEI-CDs/ Cu^{2+} system.⁹¹ Reproduced by permission from ref. 84, copyright 2012, American Chemical Society; ref. 89, copyright 2014, American Chemical Society and ref. 91, copyright 2014, Royal Chemical Society.

selectively capture Cu^{2+} to form absorbent complexes at the surfaces of CDs. As a result, the bright blue PL emission of the BPEI-CDs was quenched via an inner filter effect (Figure 7a).⁸⁴ A similar work was carried out by Salinas-Castillo and coworkers.⁸⁵ The authors found that the quenching effect of Cu^{2+} on the PL of their obtained PEI-CDs included both static (inner filter effect) and dynamic quenching mechanisms. The viewpoint was also agreed by Qu and coworkers.⁸⁶ In their experiment, the CDs obtained from chemical oxidation of GO was further treated hydrothermally in ammonia solution to synthesize amino-functionalized CDs. The amino-functionalization not only enhanced PL of CDs (PLQY was increased from 2.5% to 16.4%), but also made the PL of CDs be selectively quenched by Cu^{2+} . Tian et al. modified the CDs obtained from electrochemical treatment of graphite rods using amino TPEA ([N-(2-aminoethyl)-N,N,N'-tris(pyridin-2-ylmethyl) ethane-1,2-diamine], AE-TPEA), which was used as a model recognition unit for Cu^{2+} .⁸⁷ Liu et al. synthesized CDs by thermal treating the mixture of CA and N-(β - aminoethyl)- γ -aminopropyl methyldimethoxysilane.⁸⁸ The obtained CDs carried a large amount of ethylenediamine groups, which could recognize Cu^{2+} . Although the quenching mechanism is still not very clear, the PL emission of the modified CDs could be selectively and sensitively quenched by Cu^{2+} .

Many of the obtained amino group functionalized CDs could be used directly as PL probes for signal-off detection of Cu^{2+} in both environmental water samples and biological samples. For example, Chi et al. applied the obtained BPEI-CDs for Cu^{2+} detection in aqueous samples.⁸⁴ The methodology could offer a rapid, reliable, and selective detection of Cu^{2+} with a dynamic range from 10 to 1100 nM and a detection limit of 6 nM. Furthermore, to improve

the detection sensitivity for Cu^{2+} , BPEI-CDs were encapsulated in zeolitic imidazolate framework materials (ZIF-8), which could selectively accumulate cations (Figure 7b).⁸⁹ As a result, the dynamic range changed to 2-1000 nM, and the detection limit was significantly decreased to 80 pM. The sensors have been successfully applied for the detection of Cu^{2+} in real samples, such as river water samples, suggesting their promising applications in environmental monitoring.

Tian et al. applied their obtained amino group functionalized CDs as PL probes for Cu^{2+} in a linear range from $\sim 10^{-6}$ - 10^{-4} M at pH 4.0-9.0.⁸⁷ Furthermore, the probes exhibited good photostability and could be applied in the intracellular sensing and imaging of Cu^{2+} . In their following up work, the functionalized CDs were hybridized with CdSe/ZnS quantum dots (QDs) emitting red PL to form dual-emission fluorophores, in which QDs embedded in silica shells gave a reference PL signal for providing built-in correction to avoid environmental effects (Figure 8a).⁹⁰ The obtained dual emission hybrid probes were used to develop a ratiometric PL sensor of Cu^{2+} . Also, they have been used in real-time imaging and biosensing of cellular Cu^{2+} (Figure 8b). Liu et al. also designed ratiometric PL nanosensor for Cu^{2+} detection.⁸⁸ CDs with Cu^{2+} recognition sites were covalently linked to Rhodamine B-doped silica nanoparticles through silylation reaction without any other surface functionalization. The dual-emission nanohybrids have been used for Cu^{2+} determination in real water samples and Cu^{2+} imaging in cells. Salinas-Castillo et al. and Sun et al. also reported that their obtained CDs could be used for intracellular sensing and imaging of Cu^{2+} in biological systems.^{85,86}

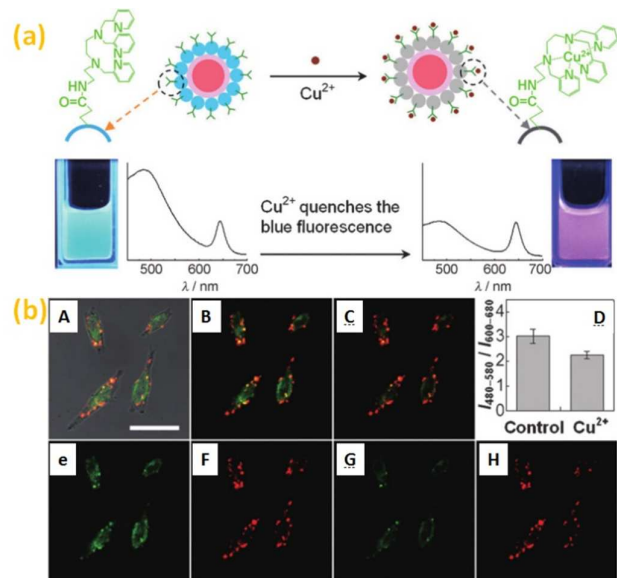


Figure. 8 (a) Dual-emission fluorescent sensing of Cu^{2+} ions based on a CdSe@CDs-TPEA nano hybrid. (b) Confocal PL images of HeLa cells before and after addition of Cu^{2+} ($100 \mu\text{M}$). Panel (A) overlay of bright-field and PL images. Panels (B) and (C) are the confocal PL images of HeLa cells before and after the exogenous Cu source treatment. (D) A bar graph showing the integrated intensity from 480–580 nm over the integrated PL intensity from 600–680 nm. Panels (E) and (G) are the confocal PL images obtained from 480–580 nm before and after the exogenous Cu source treatment, whereas panels (F) and (H) are obtained from 600–680 nm. Reproduced by permission from ref. 90, copyright 2012, Wiley-VCH.

Besides direct signal-off sensors, the amino group functionalized CDs could also be used for indirect “off-on” PL sensors. For example, BPEI-CDs were used for CN^- signal-on detection.⁹¹ CN^- could combine strongly with Cu^{2+} to $[\text{Cu}(\text{CN})_4]^-$ species, preventing Cu^{2+} from being captured by the amino groups of BPEI-CDs. As a result, CN^- “turn on” the PL signal of BPEI-CDs/ Cu^{2+} system (Figure 7c). The methodology could offer a sensitive, selective, simple and rapid

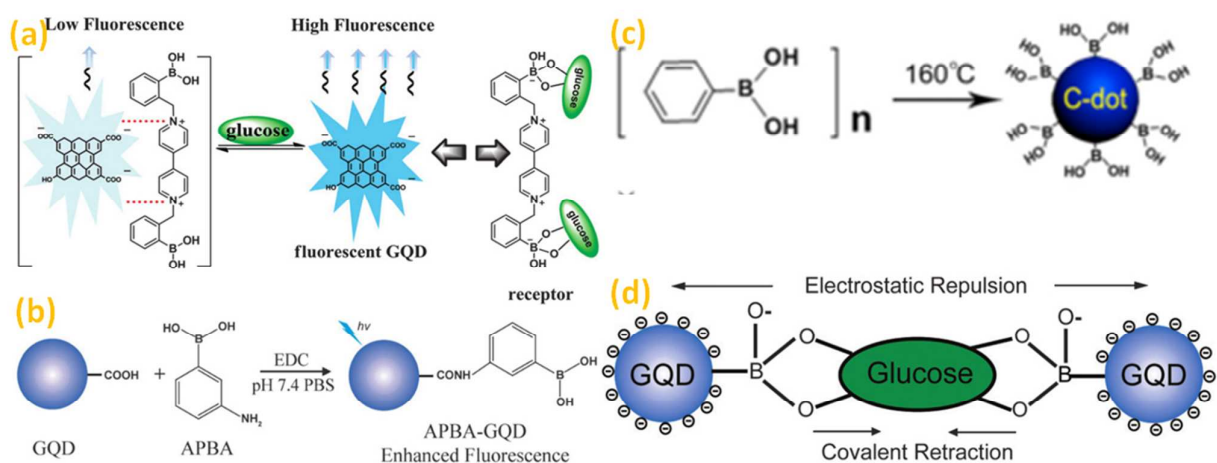


Figure 9. (a) Proposed glucose-sensing mechanism based on BBV receptor and CDs.⁹⁴ (b) Schematic representation of the functionalization of CDs with APBA.⁹⁵ (c) One-step “Synthesis-Modification Integration” strategy for fabrication of boronic Acid functionalized CDs.⁹⁶ (d) Proposed mechanism of surface quenching states (SQS) for glucose recognition.⁹⁵ Reproduced by permission from ref. 94, copyright 2013, Royal Chemical Society; ref. 95, copyright 2013, Royal Chemical Society and ref. 96, copyright 2014, American Chemical Society.

method for CN^- detection with a detection limit of $0.65 \mu\text{M}$ and a linear response range of 2 to $200 \mu\text{M}$.

2.5 PL sensors based on the interactions between thiol group functionalized CDs and heavy metal ions

Esteves da Silva and coworkers modified the CDs obtained by direct laser ablation of carbon targets with NH_2 -polyethylene-glycol (PEG_{200}) and N-acetyl-L-cysteine (NAC), which is a metabolite of the sulfur-containing amino acid.⁹² It was found that the PL of the obtained functionalized CDs could be quenched by Hg^{2+} and Cu^{2+} . Static quenching mechanisms were proposed for the phenomenon, i.e. the formation of very stable complexes between NAC residues (sulfhydryl) on the surfaces of the CDs and Hg^{2+} or Cu^{2+} . The authors proposed that the obtained CDs could be used in the detection of Hg^{2+} . Furthermore, they constructed an optical fiber sensor for Hg^{2+} in aqueous solution based on immobilizing the modified CDs in sol-gel.⁹³ Wee et al. found that the PL of CDs synthesized from Bovine serum albumin by dehydration with concentrated H_2SO_4 could be selectively quenched by Pb^{2+} .⁶³ It was supposed that the PL quenching should be caused by the electron transfer between the CDs and Pb^{2+} . Then a sensor for Pb^{2+} was developed with a limit of detection of $5.05 \mu\text{M}$.

2.6 PL sensors based on the interactions between boronic acid-functionalized CDs and glucose

In 2013, Qiu et al. developed a label-free signal-on sensor for the detection of glucose based on the PL recovery of CDs (Figure 9a). In principle, cationic boronic acid-substituted bipyridinium salt (BBV) was used to quench the PL signal of anionic CDs based on the electrostatic interaction and the electron transfer between the excited CDs and the bipyridinium. Subsequently, the addition of glucose made the boronic acids converted to more tetrahedral anionic glucoboronate esters, which could effectively neutralize the net charge of the cationic bipyridinium. As a result, the quencher was removed from the immediate vicinity of the CDs, leading to the recovery of PL signal. There was a linear relationship between the recovered PL intensity of CDs and the concentration of glucose from 1 to 60 mM.⁹⁴ The performance of the signal on sensor was not so

Journal Name

ARTICLE

good, but the FL signal change could be visually observed by naked eyes. Some researchers developed signal-off sensors for the detection of glucose based on boronic acid-functionalized CDs. Qu et al. modified the CDs from hydrothermal treatment of GO with 3-Aminobenzeneboronic acid (APBA).⁹⁵ The functionalization made the PLQY of CDs be increased greatly, from ~2.9% to 49.7%. Moreover, the obtained APBA exhibited a rapid and stable response to glucose in aqueous solution (Figure 9b). It was proposed that APBA-CDs were crosslinked by covalent anchored glucose, leading to the aggregation of APBA-CDs and efficient PL quenching. Shen et al. developed a simpler and more straight-forward method to synthesize boronic acid-functionalized CDs by hydrothermal treatment of phenylboronic acid (Figure 9c).⁹⁶ The obtained functionalized CDs also exhibited a similar response to glucose due to the same mechanism mentioned above (Figure 9d). Both of the two signal-off methods exhibited good performances. Particularly, in the latter case, the PL intensity decreased linearly over a wide glucose concentration range (from 9 to 900 μM), and had a low detection limit of 1.5 μM . Furthermore, the sensor has been applied in the detection of glucose in human serum.

2.7 PL sensors based on combining CDs with other nanomaterials

Shi et al. reported a dual-mode nanosensor with both colorimetric and fluorometric readout based on CDs and gold nanoparticles (AuNPs) for discriminative detection of GSH over Cys and Hcy (Figure 10a).⁹⁷ CDs synthesized by the microwave treatment of CA

and 2,20-(Ethylene-dioxy) bis(ethylamine) could combine with AuNPs due to electrostatic interaction, leading to the aggregation of AuNPs and CDs. Then the colour of AuNPs changed from red to blue, while the PL of CDs was quenched. GSH was found to be able to prevent AuNPs and CDs from aggregating for the multi-dentate anchor and the specific steric structure existing in GSH, and thus strong affinity of GSH to AuNPs. As a result, the color change and PL signal recovery happened. The proposed nanosensor had a detection limit of 50 nM and could discriminatively detect GSH over competitive biothiols such as Cys, Hcy and GSSG. Dai et al, developed a “turn-on” PL sensor for melamine based on melamine-induced decrease of the FRET efficiency between AuNPs and CDs (Figure 10b). It was found that CDs were prone to get close to the surfaces of AuNPs, resulting in PL quenching. However, melamine could compete with CDs due to the contained amino groups, leading to the restoration of the PL.⁹⁸ There was a good linear relationship between the recovered PL intensity and the concentration of melamine from 50 to 500 nm.

Qu and coworkers developed a signal-on sensor for K^+ based on aminated CDs and 8-crown-6 (18C6E) functionalized reduced GO (rGO).⁹⁹ In principle, the PL emission of CDs was quenched by rGO due to the tight binding of primary alkyl-ammonium with 18C6E, which induced the fluorescence resonance energy transfer (FRET). However, the FRET process was inhibited because of competition

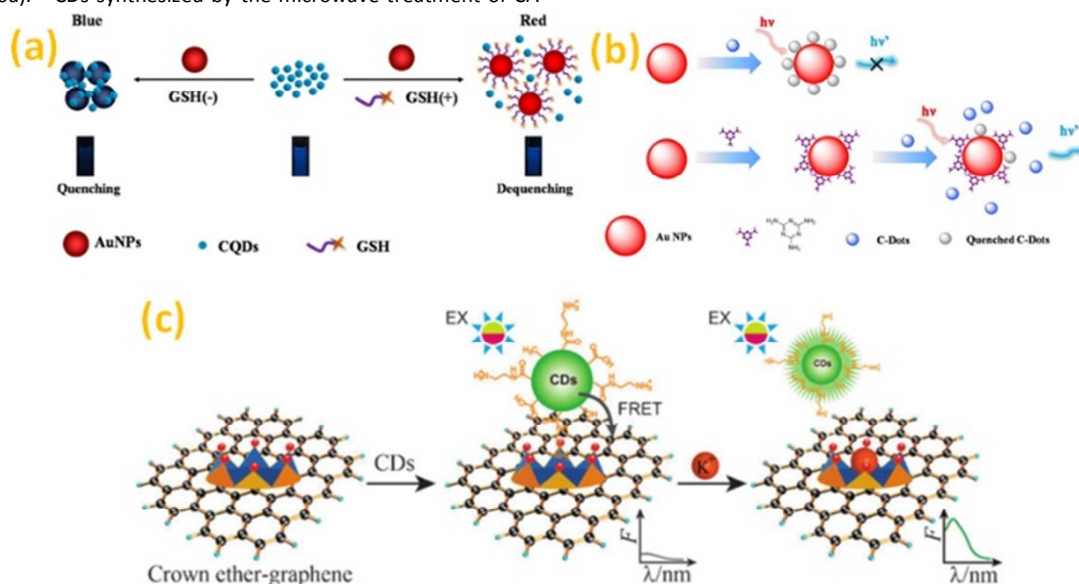


Figure 10. (a) Schematic principle of GSH detection by using the dual-mode nano-sensor with both colorimetric and fluorometric readout.⁹⁷ (b) Mechanism for the detection of melamine based on FRET between CDs and AuNPs.⁹⁸ (c) Schematic illustration of the FRET model based on CDs-graphene and the mechanism of K^+ determination.⁹⁹ Reproduced by permission from ref. 97, copyright 2014, Elsevier; ref. 98, copyright 2014, Elsevier and ref. 99, copyright 2012, Royal Chemical Society.

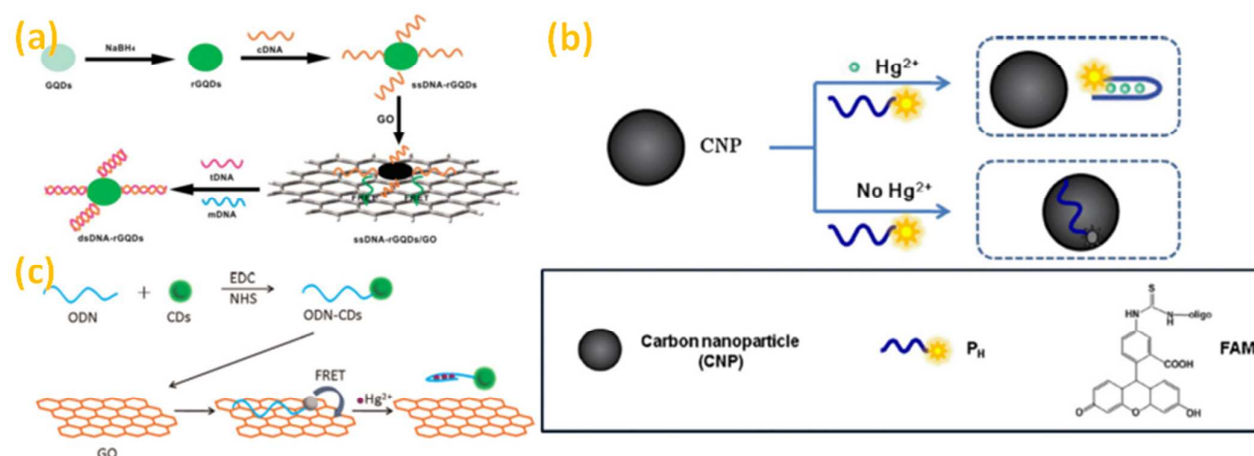


Figure 11. (a) Schematic illustration of a universal PL sensing platform for the detection of DNA based on FRET between CDs and GO.¹⁰⁰ (b) A schematic (not to scale) illustrating the CDs-based Hg²⁺ detection based on conformational change of a Hg²⁺-specific T-rich OND (PH). PH: a FAM-labeled Hg²⁺-specific OND probe.¹⁰² (c) Schematic illustration of the GO-based sensor system for Hg²⁺ detection.¹⁰³ Reproduced by permission from ref. 100, copyright 2014, Royal Chemical Society; ref. 102, copyright 2011, Elsevier and ref. 103, copyright 2015, Elsevier.

between K⁺ and ammonium for 18CGE, leading to a recovered PL signal (Figure 10c).

2.8 PL sensors based on combining CDs with DNA techniques

CDs have been combined with DNA techniques to develop novel PL signal on system for sensing. For example, Feng et al. developed two DNA sensors with CDs.¹⁰⁰ In their work, CDs were reduced with NaBH₄, and subsequently connected with single-stranded DNA linear response range of 6.7–46.0 nM, with a detection limit of 75.0 pM. In their another work, carbon nanotubes were used instead of GO to quench the PL of CDs.¹⁰¹ As expected, similar results were obtained. Some other researchers developed CDs-based biosensing systems for Hg²⁺. In one of Sun's works, poor PL CDs from candle soot were used to quench the PL of dye-labeled T-rich ssDNA via π - π stacking interactions between DNA bases and CDs.¹⁰² Subsequently, the quenched PL signal was recovered by Hg²⁺ due to the formation of T-Hg²⁺-T induced hairpin (Figure 11b). Accordingly, the PL intensity increased with the concentration of Hg²⁺ in the range from 50 to 250 nM, with a detection limit of 10 nM. Cui and coworkers also developed a PL sensor for Hg²⁺ accordingly to a similar principle mentioned in Sun's work. Differently, they used a high PL CDs as the PL emitter, while GO as the PL quencher (Figure 11c).¹⁰³ A linear relationship was obtained between relative PL intensity and the concentration of Hg²⁺ in the range of 5–200 nM, and the detection limit was 2.6 nM.

2.9 PL sensors based on combining CDs with immunological techniques

Zhu et al. developed a PL immunoassay based on CDs for the detection of human immunoglobulin G (IgG, antigen).¹⁰⁴ In principle,

(ssDNA). The PL signal of the ssDNA-rCDs probe could be substantially quenched by GO after being absorbed on the surfaces of GO through electrostatic attractions and π - π stacking interactions. After being hybridized with target DNA, the PL probes were detached and liberated from GO, leading to the PL recovery (Figure 11a). The established method for DNA detection had a

carboxyl functionalized CDs were conjugated with goat antihuman IgG (gIgG, antibody), without any obvious change in PL property (Figure 12a). The specific interaction between gIgG and IgG was found to be able to enhance the PL intensity of the CDs-gIgG conjugate, which was explained by the decrease of surface defects of CDs-COOH. Zhao and coworkers proposed another immunosensor for IgG (Figure 12b).¹⁰⁵ In brief, mouse antihuman immunoglobulinG (mIgG, antibody) labelled CDs and GO were brought into FRET proximity due to the π - π stacking interaction between CDs and GO and the nonspecific binding interaction between mIgG and the GO surface. Accordingly, the PL emission of the labelled CDs was quenched by GO. However, after binding to IgG (antigen) due to the specific antibody-antigen interaction, the distance between labelled CDs and GO surface was effectively increased, resulting in a PL recovery. The PL intensity increased with increasing concentration of human IgG in the range from 0.2 to 12 mg mL⁻¹, with a detection limit of 10 ng mL⁻¹. Du et al. designed an immunosensor for 4, 4'-biphenyl diphenyl (PBB15) detection based on FRET between CDs and AuNPs.¹⁰⁶ The CDs were labelled with 4,4'-dibrominated biphenyl antigen (PBBAg) while the AuNPs were modified with anti-PBB15 antibody (antiPBBAb). The specific combination of the functionalized CDs and AuNPs led to a

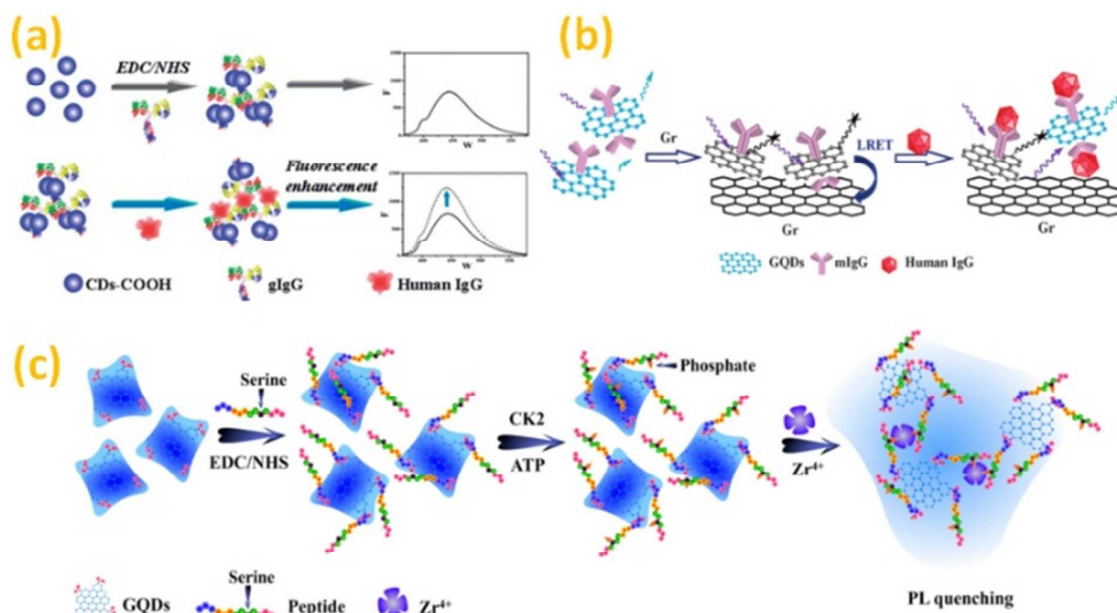


Figure 12. (a) Schematic illustration for the detection mechanism of human IgG using the carboxyl-functionalized CDs.¹⁰⁴ (b) Schematic illustration of a universal immunosensing strategy based on regulation of the interaction between GO and CDs.¹⁰⁵ (c) Schematic Representation of the CK2 Kinase Assay Based on the Aggregation and PL Quenching of Phosphorylated Peptide-CD Conjugates via Zr⁴⁺ Ion Linkages.¹⁰⁷ Reproduced by permission from ref. 104, copyright 2014, Royal Chemical Society; ref. 105, copyright 2013, Royal Chemical Society and ref. 107, copyright 2013, American Chemical Society.

significant quenching on the PL of CDs due to FRET. However, PBBAg-CDs could be partly displaced from antiPBBAb-AuNPs by PBB15 due to the competitive immunoreaction, producing a recovered PL signal. The increased PL intensity was proportional to the concentration of PBB15 in the range of 0.05–4 $\mu\text{g mL}^{-1}$, with a detection limit of 0.039 $\mu\text{g mL}^{-1}$. Wang et al. reported a PL assay for the activity of a protein kinase (Figure 12c).¹⁰⁷ CDs were covalently conjugated with serine-containing peptide, which was subsequently phosphorylated by Ser/Thr-specific protein kinase casein kinase II (CK2) in the presence of adenosine 5'-triphosphate (ATP). Then the functionalized CDs aggregated as Zr⁴⁺ ions were introduced according to a similar mechanism mentioned in other works.^{55,56} As a result, the PL of CDs was quenched.

2.10 PL sensors based on interactions between CDs and some organics

Gayuela et al. found that the CDs passivated with acetone could be used for the detection of 2,4-dinitrophenol (DNP) at pH 3.5 and for 2-amino-3,4,8-trimethyl-3H-imidazo[4,5-f]quinoxaline (4,8-DiMeIQx) at physiological pH.¹⁰⁸ The authors claimed that the protonated DNP may interact with oxygenated surface of CDs by hydrogen bonding, causing the observation of PL quenching. Costas-Mora et al. found that the PL signal of PEG-passivated CDs could be selectively quenched by methylmercury.¹⁰⁹ It was proposed the

hydrophobic methylmercury could easily cross the PEG coating and came into contact with CDs, while hydrophilic ions could not behave in this way with CDs. Accordingly a sensitive PL sensor was developed for methylmercury, with a detection limit of 5.9 nM. Li et al. developed a molecularly imprinted PL sensor for the determination of dimethoate based on the FRET between methyl red (MR) and CDs.¹¹⁰ A doped molecular template polymer was prepared by electropolymerization. During dimethoate detection, a competitive reaction occurred between dimethoate and CDs-labeled dimethoate, leading to PL inhibition. There was a good linear PL response for dimethoate over the concentration range from 6.0×10^{-10} to 3.4×10^{-8} mol L⁻¹, with a detection limit of 1.83×10^{-11} mol L⁻¹.

3. ECL sensor

Electrochemiluminescence (ECL) is a kind of luminescence produced during electrochemical reactions in solutions. ECL is an important sensing technique for its combining the merits of chemiluminescence and electrochemistry, and thus showing many distinct advantages including high signal-to-noise ratio, easy light-emission control, high sensitivity and selectivity, and wide response range.¹¹¹ Accordingly, since the ECL activities of CDs were first

discovered by Chi et al.,¹¹² more and more attention has been paid to ECL researches of CDs, especially ECL sensing based on CDs. The first reported ECL of CDs was based on CD/S₂O₈²⁻ coreactant system, which produced strong and stable cathodic ECL signal (Figure 13a). It was proposed that CDs could be electro-reduced into negatively charged CDs (R⁻), while S₂O₈²⁻ could be reduced into SO₄⁻ free radicals. The electron transfer annihilation R⁻ between and SO₄⁻ produced excited-state CDs (R^{*}), which gave strong emission when came back to the ground state (Figure 13b). Up to date, many ECL sensors have been developed based on the CD/S₂O₈²⁻ coreactant ECL system. For example, it has been applied in the detection of Cd²⁺ and Cr(VI). Li et al. found that the ECL signal of CDs/S₂O₈²⁻ could be quenched obviously by some metal ions due to the fact that the interaction between the metal ions and the oxygen-containing functional groups (e.g. hydroxyl and carboxyl groups) at the surfaces of CD led to the aggregation of CDs.¹¹³ In the work, Cys was used as an effective masking agent to eliminate the interferences of other metal ions during determining Cd²⁺. Dong et al. found that the ECL signal of CDs/S₂O₈²⁻ system could also be quenched by Cr(VI), which mainly existed in the form of metal anion (CrO₄²⁻).¹¹⁴ The authors proposed a dynamic mechanism for the quenching behaviors of Cr(VI) based on their experimental results (Figure 13c). To establish a selective ECL sensor for Cr(VI), EDTA was added to mask all metal cations. The developed ECL sensor showed a wide linear response range from 50 nM to 60 μM, with a detection limit of 20 nM. Furthermore, the sensor has shown a good practicability for its successful application in the detection of Cr(VI) in a river water sample. Lu et al. developed a "off-on" DNA ECL sensor (Figure 13d).¹¹⁵ It was found that ssDNA modified AuNPs (AuNPs-ssDNA) could bind CDs non-covalently, leading to the quenching in ECL signal due to the ECL resonance energy transfer between CDs and AuNPs. However, the non-covalent interaction between CDs and AuNPs could be weakened as AuNPs-ssDNA was hybridized with target DNA. Accordingly, the ECL intensity increased

linearly as the concentration of the target DNA increased from 25 to 400 nM, with a detection limit of 13 nM.

More works on ECL of CDs were carried out by hybridizing CDs with some other nanomaterials, facilitating the immobilization on working electrodes and the bio-modifications. For example, Yang et al. prepared CDs/GR hybrid by hydrothermally treating the mixture of CDs and GO.¹¹⁶ Then the obtained nanohybrids were modified on a titanium ribbon working electrode for the detection of pentachlorophenol (PCP), which was considered to be able to react with the excited-state CDs. The developed sensor showed a wide linear range from 1.0×10⁻¹² to 1.0×10⁻⁸ mol L⁻¹ with a detection limit of 1.0×10⁻¹² mol L⁻¹. Some biosensors have been developed based on the ECL of CDs/S₂O₈²⁻ system. For example, Zhang et al. immobilized carboxyl groups-containing CDs on the surface of amine-functionalized Au/SiO₂ core-shell nanoparticles to form Au/SiO₂/CDs hybrid for the detection of 8-hydroxyl-2'-deoxyguanosine (8-OHdG).¹¹⁷ The nanohybrid was modified on a Pt working electrode, which was subsequently functionalized with rabbit anti-8-OHdG (Ab) before use for the detection of 8-OHdG. It was proposed that the ECL intensity of the modified electrode would be decreased as the electron transfer on the electrode surface was hindered. Accordingly, the ECL intensity of the modified electrode decreased as 8-OHdG was bound on the electrode surface by the specific interaction between Ab and 8-OHdG. Under optimal conditions, the authors developed an ECL immunosensor for 8-OHdG with a wide linear range from 0.2 to 200 ng mL⁻¹ and a low detection limit of 0.085 ng mL⁻¹. Yu et al. reported a sensitive sandwich-type immunosensor for prostate protein antigen (PSA).¹¹⁸ First, a glassy carbon electrode was modified with the nanohybrid of 3D graphene and AuNPs (3D-GR@AuNPs) followed by incubation with the primary anti-PSA (Ab₁). Then, CDs were hybridized with nanoporous silver (NPS) by sonication into NPS@CDs composite, which was subsequently labelled with the secondary anti-PSA (Ab₂).

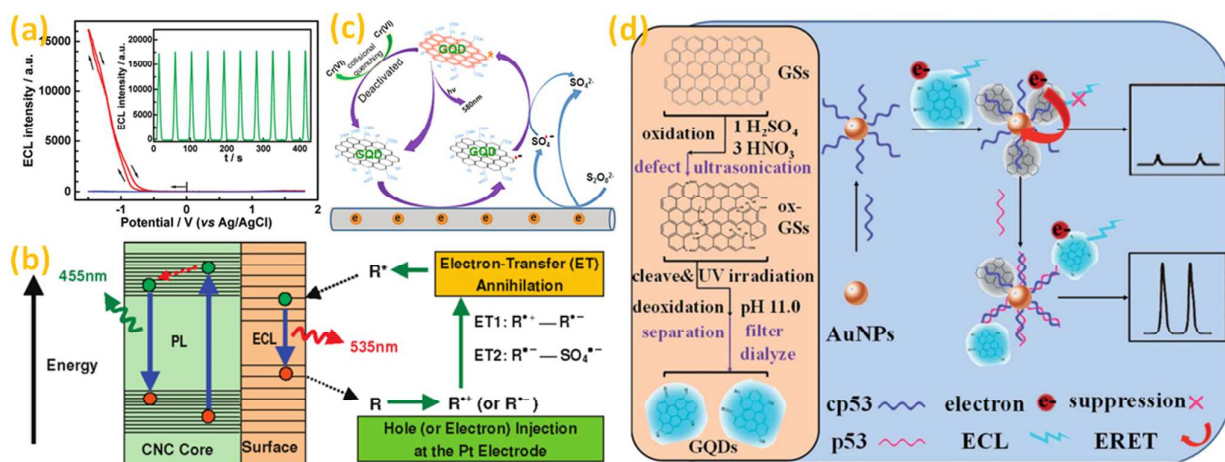


Figure 13. (a) ECL responses of the CDs in the absence (blue line) and presence (red line) of 1 mmol L⁻¹ K₂S₂O₈; Inset: ECL responses of CDs - S₂O₈²⁻ system obtained during a continuous potential scan between -1.5 and +0.75 V.⁷⁰ (b) Schematic illustration of the ECL and PL mechanisms in CDs.¹¹² (c) ECL reaction mechanism of the CD/S₂O₈²⁻ system in the presence of Cr(VI).¹¹⁴ (d) Schematic representation of the preparation of CDs and the biosensing mechanism, by an AuNP-induced ECL quenching of the CDs.¹¹⁵ Reproduced by permission from ref. 70, copyright 2010, American Chemical Society; ref. 112, copyright 2009, American Chemical Society; ref. 114, copyright 2015, Elsevier and ref. 115, copyright 2014, Royal Chemical Society.

The specific interaction between PSA and anti-PSA made NPS@CDs bound on the surface of the modified GCE, producing a strong cathodic ECL signal in the presence of $S_2O_8^{2-}$ (Figure 14a). The biosensor displayed good performance for the detection of PSA in the range from 1 to 50 $\mu\text{g mL}^{-1}$, with a low detection limit of 0.5 $\mu\text{g mL}^{-1}$. In another work of them, a similar strategy was proposed for the detection of Michigan cancer foundation-7 (MCF-7) human breast cancer cells.¹¹⁹ In brief, GCE modified with 3D-GR@AuNPs was used to capture cancer cells due to its high surface area-to-weight ratio and excellent mechanical properties. CDs coated mesoporous silica nanoparticles (CDs@MSNs) were conjugated with DNA aptamers targeting mucin1 (MUC1), which is a glycoprotein expressed on the apical surface of epithelial cells and whose overexpression is often associated with some kinds of cancers. Accordingly, in the presence of MCF-7 cells, CDs@MSNs were captured by the modified GCE, producing strong ECL emission in the presence of $S_2O_8^{2-}$ (Figure 14b). The developed method showed a good analytical performance for the detection of MCF-7 cancer cells

ranging from 500 to 2×10^7 cells mL^{-1} with a detection limit of 230 cells mL^{-1} . The authors also hybridized CDs with ZnO nanospheres to obtain ZnO@CDs hybrid and used them for the detection of leukemia cells, according to a similar principle for the detection of MCF-7 cells (Figure 14c).¹²⁰ Therefore, similar sensing performances were obtained. Lou and coworkers developed a signal-off ECL sensor for DNA detection based on site-specific cleavage of *Bam*HI endonuclease.¹²¹ In the sensor fabrication (Figure 14d), CS_2 functionalized probe DNA was assembled on gold electrode (GE) via bidentate chelation (S–Au–S bonds), and CDs with abundant carboxyl groups were bound to the carboxylated end of the probe DNA using ethylenediamine as the binder to generate ECL signal. After being hybridized with target DNA, the formed dsDNA was cleaved by *Bam*HI endonuclease, leading to the decrease of ECL intensity. The authors claimed that the signal of ECL sensor exhibited a linear range from 5 fM to 100 pM with a detection limit of 0.45 fM.

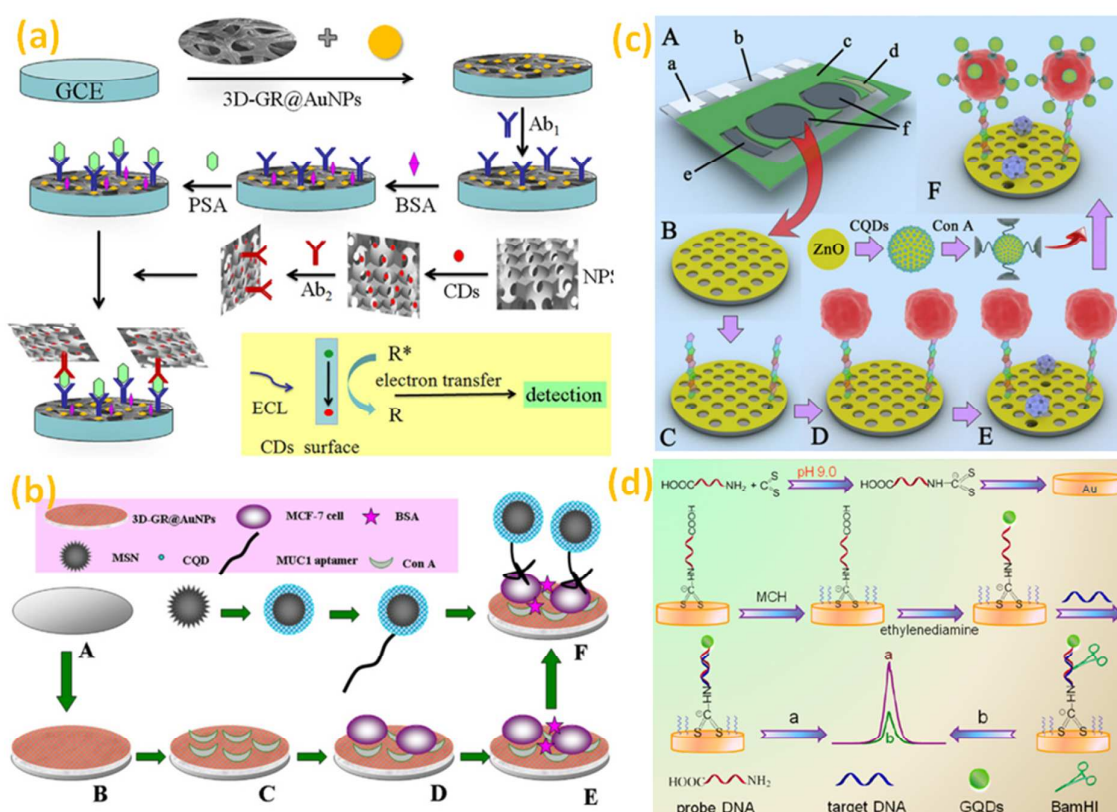


Figure 14. (a) Schematic representation of the fabrication process of the PSA immunosensor.¹¹⁸ (b) The fabrication process of the ECL cytosensor.¹¹⁹ (c) Schematic representation of the assay procedure for the ECL device.¹²⁰ (d) Schematic illustration of the ECL biosensor based on CDs combined with endonuclease cleavage and bidentate chelation.¹²¹ Reproduced by permission from ref. 118, copyright 2013, Elsevier; ref. 119, copyright 2014, Elsevier; ref. 120, copyright 2013, Elsevier and ref. 121, copyright 2015, American Chemical Society.

Journal Name

ARTICLE

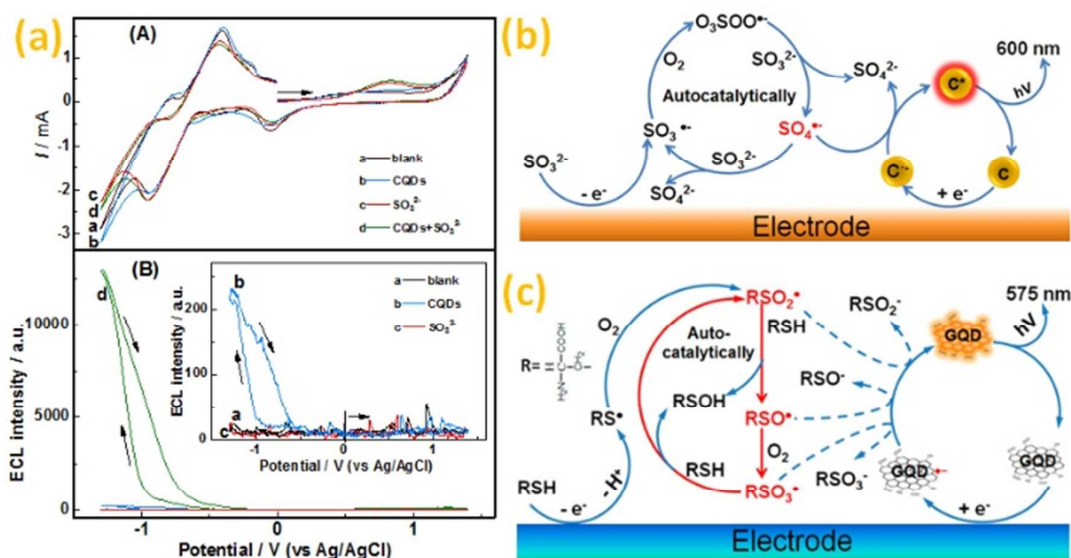


Figure 15. (a) Cyclic voltammogram (A) and the corresponding ECL potential curves (B) of CDs in the absence and presence of SO_3^{2-} . (b) ECL mechanism of CD/ SO_3^{2-} system.¹²² (c) ECL mechanism of CD/L-Cys system.¹²³ Reproduced by permission from ref. 122, copyright 2013, Elsevier and ref. 123, copyright 2014, American Chemical Society.

Besides CD/ $\text{S}_2\text{O}_8^{2-}$ system, CD/ SO_3^{2-} system was subsequently found by Chi and coworkers to produce strong and stable cathodic ECL signal (Figure 15a).¹²² However, a previous anodic polarization of SO_3^{2-} and the presence of dissolved oxygen (O_2) were both necessary for producing the cathodic ECL signal. The authors studied and proposed the ECL mechanism the CD/ SO_3^{2-} system in detail (Figure 15b). In brief, SO_3^{2-} was oxidized in the anodic polarization into sulfur trioxide anion free radicals ($\text{SO}_3^{\cdot-}$), which subsequent initiated a three-step auto-catalytic reaction in the presence of dissolved oxygen (O_2), producing $\text{SO}_4^{\cdot-}$ all the time. In the following cathodic polarization process, the electron transfer between $\text{SO}_4^{\cdot-}$ and the electro-generated R^{\cdot} produced R^* , which gave rise to the strong ECL emission when going back to the ground state. The CD/ SO_3^{2-} system itself could be used for sensing SO_3^{2-} and SO_2 since there was a good linear relationship between the ECL intensity and the concentration of SO_3^{2-} in the range of 1.0×10^{-5} to 1.0×10^{-3} mol L^{-1} . However, the further sensing applications of CD/ SO_3^{2-} system have not been reported. Chi et al. also developed CD/L-Cys ECL sensing system, the analytical performance was quite similar with that of the above mentioned CD/ SO_3^{2-} system (Figure 16c).¹²³ The electrochemical oxidation of L-Cys (RSH) produced a free radical intermediate (RO^{\cdot}), which was further oxidized to RSO_2^{\cdot} by O_2 dissolved in the solution. Subsequently, the formed RSO_2^{\cdot} initiated a three-step autocatalytic reaction, in which three kinds of free radicals (RSO^{\cdot} , RSO_2^{\cdot} , and RSO_3^{\cdot}) were produced continuously. These free radicals reacted with electro-generated R^{\cdot} in the

following cathodic polarization process, producing excited-state CDs that producing strong ECL signal. The CDs/L-Cys system was used for the selective detection of Pb^{2+} . It was proposed that Pb^{2+} itself or its complexation with L-Cys could inhibit the formation of the free radicals (RSO^{\cdot} , RSO_2^{\cdot} , and RSO_3^{\cdot}) by the oxidation of L-Cys, then blocked the formation of R^* . The new methodology could offer a rapid, reliable, and selective detection of Pb^{2+} with a detection limit of 70 nM and a dynamic range from 100 nM to 10 μM . Furthermore, the sensor was successfully applied in monitoring Pb^{2+} in a local river.

As has been discussed above, the cathodic ECL properties of CDs have been well studied and applied in sensing. However, much less attention has been paid to the anodic ECL of CDs. Yu and coworkers reported that the CDs from hydrothermal treatment of GO produced anodic ECL signal in the presence of H_2O_2 .¹²⁴ It was proposed that the anodic ECL signal was caused by the electron transfer between the electro-generated $\text{R}^{+\cdot}$ and $\text{O}_2^{\cdot-}$ formed by the electro-oxidation of H_2O_2 . The developed CD/ H_2O_2 coreactant ECL system was applied for ATP determination. The carboxyl group-containing CDs were covalently combined with the amino-functionalized SiO_2 nanoparticles to form SiO_2/CDs composites, which were subsequently incubated with an amino group functionalized ssDNA (ssDNA2). At the same time, another thiol-functionalized ssDNA (ssDNA1) was modified on the gold working electrode. Thus, SiO_2/CDs were captured by the modified electrode through the interaction among ssDNA1, ATP and ssDNA2. The ECL intensity

increased linearly with the concentration of ATP in the range from 5.0×10^{-12} to 5.0×10^{-9} mol L⁻¹, with a detection limit of 1.5×10^{-12} mol L⁻¹. The observed anodic ECL mentioned above seems to be a special case for CDs without any modification. Chi and coworkers synthesized hydrazide-modified CDs (HM-CDs), which could produce an anodic ECL signal similar with luminol (Figure 16a).¹²⁵ CDs from chemical oxidation of XC-72 carbon black were refluxed with hydrazine.⁷¹ It was proposed that the obtained HM-CDs contained a lot of luminol-like units due to the reaction between the carboxylated CDs and N₂H₄ (Figure 16b).¹²⁶ In alkaline solutions, HM-CDs produced a strong ECL signal with the peak at around +0.72 V. Furthermore, the anodic ECL signal could be enhanced greatly by H₂O₂. The ECL intensity increased linearly with the concentration of H₂O₂ in a wide range of 3 to 500 μM, with a detection limit of 0.7 μM.

4. CL sensors

CL is the emission of light resulting from a redox chemical reaction. As an analytical technique, CL usually shows advantages including high sensitivity, wide response range, simple instrumentation, and free of background scattering light interference. Therefore, the CL properties of CDs have also attracted increasing research interests. In 2010, Dong et al. first observed the CL behaviors of CDs from hydrothermal treatment of HOCH₂CH₂OCH₂CH₂NH₂ and CA.⁷⁰ During investigating the ECL behaviors of the CDs in the presence of K₂S₂O₈, a strong background emission signal was observed. It was supposed that the light emission background should be CL. Unfortunately, there was no more investigation on CL properties of the CDs given by the authors.

Up to now, many CD-based CL systems have been developed. In general, these CL systems involved some strong oxidants, such as MnO₄⁻, Ce(IV) and some free radicals.¹²⁷⁻¹³⁰ The first sensor based on the CL of CDs was developed by Lin and coworkers. It was found that the CDs from microwave treatment of glycerine and PEG mixture could produce strong CL emission in the presence of NaNO₂ and H₂O₂.¹²⁹ It was suggested that the CL of CDs should be attributed to the surface states based on emission spectrum data. An annihilation mechanism was proposed for the CL of the CD/NaNO₂/H₂O₂ system (Figure 17a). The mixing of NaNO₂ and acidified H₂O₂ produced ONOOH and OH[•], which served as the hole

injectors to convert CDs into R^{•+}. On the other hand, ONOOH reacted with H₂O₂ in acidic solution to form O₂^{•+}, which changed CDs into R^{•-}. The electron-hole annihilation of R^{•+} and R^{•-} resulted in the energy release with CL emission. Furthermore, a sensitive CL sensor for nitrite was developed based on the CD/NaNO₂/H₂O₂ system. The CL intensity increased linearly as nitrite concentration was increased from 1.0×10^{-7} to 1.0×10^{-5} M, with a detection limit of 5.3×10^{-8} M. The sensor showed good practicability, and has been applied for the detection of nitrite in real samples, such as pond water, river water, and milk. The authors also developed a CD/H₂O₂/NaHSO₃ system (Figure 17b),¹³⁰ with a similar CL mechanism to those of the CD/NaNO₂/H₂O₂ system. However, the system was not further applied in sensing. Shi et al. developed a selective CL sensing system for the detection of Co²⁺ based on the CDs/Co²⁺/H₂O₂/OH⁻ system (Figure 17c).¹³¹ Co²⁺ ions were adsorbed on the surface of CDs, then catalyzed the dissociation of H₂O₂ through a Fenton-like reaction, producing abundant OH[•] and O₂^{•-} radicals around the surface of CDs. The recombination of O₂^{•-} led to the formation of energy-rich excited singlet oxygen dimol species (O₂)₂^{*}. The latter could react with CDs to produce their excited stated (R^{*}). The constructed CL sensing system exhibited a stable response to Co(II) over the concentration range from 1.0 to 1000 nM with a detection limit as low as 0.67 nM. Amjadi et al. reported a CL sensor for uric acid based on the developed CD/Ce(IV) system.¹³² It was found that CDs from pyrolysis of CA could be oxidized by Ce(IV) to produce strong CL signal. Uric acid could quench the CL of CDs/Ce(IV) system due to the competition of uric acid with CDs for Ce(IV). The proposed CL system exhibited good analytical performance for determination of uric acid in the range of 1.0×10^{-6} to 1.0×10^{-4} M, with a limit of detection of 5.0×10^{-7} . HM-CDs synthesized by Chi et al. also exhibited excellent CL properties in the presence of O₂ in alkaline solutions, due to their contained luminol-like units (Figure 16b).¹²⁵ The CL intensity increased dramatically with the pH value in the range from pH 8-11. In air-saturated solutions, there was a good semilogarithmic correlation between the CL intensity and the pH value, suggesting a promising application in sensing OH⁻. Furthermore, the CL intensity was related to the concentration of the dissolved oxygen (O₂), suggesting that the HM-CDs could be applied in O₂ sensing.

Conclusion and future perspectives

In this review, the principles and advantages of the sensing systems based on the luminescent properties of CDs have been summarized. We have discussed PL sensors, ECL sensors and CL sensors of CDs which have been applied in chemical analysis and bioanalysis. Although great attention has been paid to CDs, the study on the sensing based on the luminescent properties of CDs are still in the initial stage. To expand the applications of CDs in sensors, some issues remain important in further studies.

1. For PL sensors, the performances would be greatly affected by the PL properties of CDs. Although some high PL CDs have been synthesized, the PLQY of most reported CDs were still incomparable with those of QDs. In particular, the PLQYs of CDs with long-wavelength (e.g. yellow and red) emission were usually less than 5%, which is unfavourable for PL sensors,

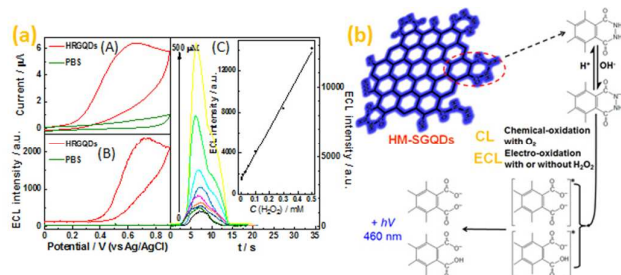


Figure 16. (a) Cyclic voltammograms (A) and ECL emission curves (B) of blank and 40 μg/mL HM-CDs in pH 9 PBS, and ECL responses of 40 μg/mL HM-SGQDs upon addition of various concentrations of H₂O₂ (C). (b) CL and ECL mechanisms of HM-CDs. Reproduced by permission from ref. 125, copyright 2014, Royal Chemical Society.

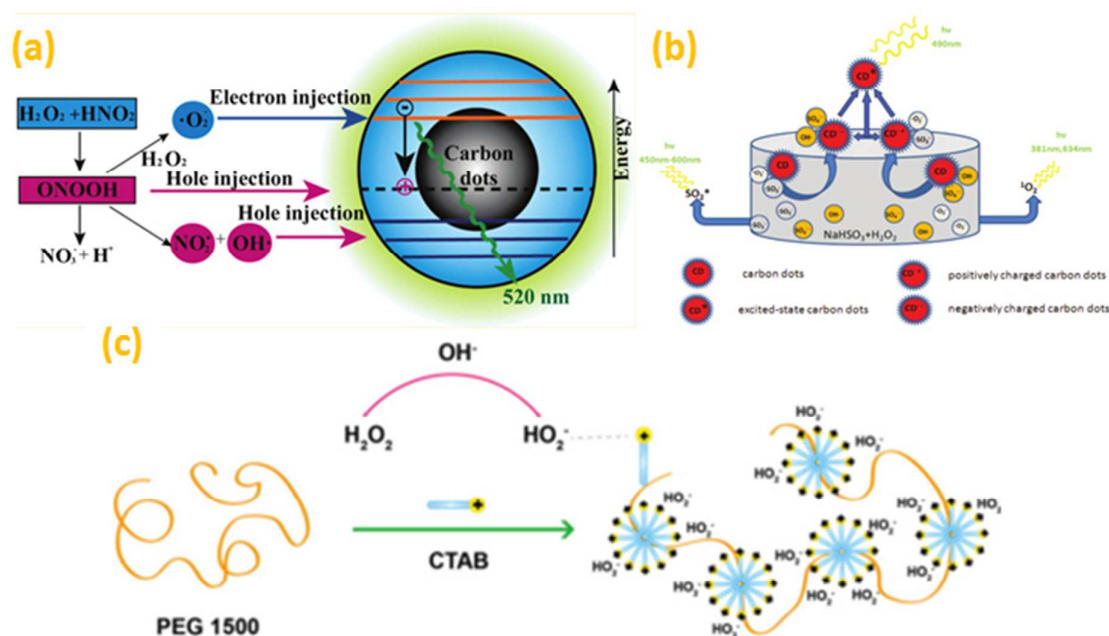


Figure 17. (a) Schematic illustration of the CL mechanism of CDs/NaNO₂/H₂O₂ system.¹²⁹ (b) CL reaction mechanism for the H₂O₂-NaHSO₃/CDs system.¹³⁰ (c) schematic illustration for the concentrating of hydroperoxyl anions in CTAB-PEG microenvironment.¹³¹ Reproduced by permission from ref. 129, copyright 2011, American Chemical Society; ref. 130, copyright 2011, American Chemical Society; and ref. 131, copyright 2013, Elsevier.

especially for intracellular sensing. Therefore, improving the PL properties of CDs is quite important and urgent.

1. For ECL sensors, only a few coreactant ECL systems have been studied and used for sensing. Developing new and excellent CDs based ECL systems are of great significance for promoting the sensing applications of CDs.
2. For CL sensors, several exciting and important researches have been carried out, but CDs based CL sensing studies and applications are still at the infant stage. Therefore, synthesis of CDs with high CL activities, studies for new CDs based CL systems and related CL mechanisms, and various CL sensing applications might be interesting research topics on CDs in near future.
3. Hybridization with other nanomaterials and conjugation with biomolecules for developing sensitive and selective biosensors would become prevalent in the applications of CDs.

Acknowledgements

This study was financially supported by National Natural Science Foundation of China (21305017, 21375020) and Specialized Research Fund for the Doctoral Program of Higher Education of China (20133514110001).

Notes and references

- 1 Y.-P. Sun, B. Zhou, W. Wang, K. A. S. Fernando, P. Pathak, M. J. Mezziani, B. A. Harruff, X. Wang, H. Wang, P. G. Luo, H. Yang, M. E. Kose, B. Chen, L. M. Veca and S. Xie, *J. Am. Chem. Soc.*, 2006, **128**, 7756-7757.
- 2 L. A. Ponomarenko, F. Schedin, M. I. Katsnelson, R. Yang, E. W. Hill, K. S. Novoselov and A. K. Geim, *Science*, 2008, **320**, 356-358.
- 3 J. Guttinger, F. Molitor, C. Stampfer, S. Schnez, A. Jacobsen, S. Droscher, T. Ihn and K. Ensslin, *Rep. Prog. Phys.*, 2012, **75**, 126502.
- 4 X. Zhou, S. Guo and J. Zhang, *ChemPhysChem*, 2013, **14**, 2627-2640.
- 5 J. L. Li, B. Tang, B. Yuan, L. Sun and X. G. Wang, *Biomaterials*, 2013, **34**, 9519-9534.
- 6 H. Sun, L. Wu, W. Wei and X. Qu, *Mater. Today*, 2013, **16**, 433-442.
- 7 M. J. Mezziani, L. Cao, S. Sahu and Y.-P. Sun, *Acc. Chem. Res.*, 2012, **45**, 176-178.
- 8 L. Lin, M. Rong, F. Luo, D. Chen, Y. Wang and X. Chen, *Trac. Trend. Anal. Chem.*, 2014, **54**, 83-102.
- 9 J. Shen, Y. Zhu, X. Yang and C. Li, *Chem. Commun.*, 2012, **48**, 3686-3699.
- 10 Z. Zhang, J. Zhang, N. Chen and L. Qu, *Energy Environ. Sci.*, 2012, **5**, 8869.

- 1
2
3
4
5
6
7
8
9
10
11
12
13
14
15
16
17
18
19
20
21
22
23
24
25
26
27
28
29
30
31
32
33
34
35
36
37
38
39
40
41
42
43
44
45
46
47
48
49
50
51
52
53
54
55
56
57
58
59
60
- 11 M. Bacon, S. J. Bradley and T. Nann, *Part. Part. Syst. Char.*, 2014, **31**, 415-428.
- 12 L. Li, G. Wu, G. Yang, J. Peng, J. Zhao and J. J. Zhu, *Nanoscale*, 2013, **5**, 4015-4039.
- 13 S. Zhu, S. Tang, J. Zhang and B. Yang, *Chem. Commun.*, 2012, **48**, 4527-4539.
- 14 X. Yan, B. Li and L.-S. Li, *Acc. Chem. Res.*, 2012, **46**, 2254-2262.
- 15 Y. Xu, J. Liu, C. Gao and E. Wang, *Electrochem. Commun.*, 2014, **48**, 151-154.
- 16 S. N. Baker and G. A. Baker, *Angew. Chem. Int. Ed.*, 2010, **49**, 6726-6744.
- 17 H. Li, Z. Kang, Y. Liu and S.-T. Lee, *J. Mater. Chem.*, 2012, **22**, 24230.
- 18 Y. Wang and A. Hu, *J. Mater. Chem. C*, 2014, **2**, 6921.
- 19 K. Hola, Y. Zhang, Y. Wang, E. P. Giannelis, R. Zboril and A. L. Rogach, *Nano. Today*, 2014, **9**, 590-603.
- 20 J. C. G. Esteves da Silva and H. M. R. Gonçalves, *Trac. Trend. Anal. Chem.*, 2011, **30**, 1327-1336.
- 21 R. a. J. Robertson, *J. Appl. Phys.*, 1996, **80**, 2998-3003.
- 22 F. Demichelis, S. Schreiter, A. Tagliaferro, *Phys. Rev. B*, 1995, **51**, 2143.
- 23 L. Cao, X. Wang, M. J. Meziani, F. L. H. Wang, P. G. Luo, Y. Lin, B. A. Harruff, L. M. Veca, D. Murray, S.-Y. Xie and Y.-P. Sun, *J. Am. Chem. Soc.*, 2007, **129**, 11318-11319.
- 24 Z. A. Qiao, Y. Wang, Y. Gao, H. Li, T. Dai, Y. Liu and Q. Huo, *Chem. Commun.*, 2010, **46**, 8812-8814.
- 25 R. Liu, D. Wu, S. Liu, K. Koynov, W. Knoll and Q. Li, *Angew. Chem. Int. Ed.*, 2009, **48**, 4598-4601.
- 26 H. Peng and J. Travas-Sejdic, *Chem Mater*, 2009, **21**, 5563-5565.
- 27 Y. Liu, C.-y. Liu and Z.-y. Zhang, *J. Colloid Interface Sci.*, 2011, **356**, 416-421.
- 28 H. Zheng, Q. Wang, Y. Long, H. Zhang, X. Huang and R. Zhu, *Chem. Commun.*, 2011, **47**, 10650-10652.
- 29 S. Zhu, J. Zhang, S. Tang, C. Qiao, L. Wang, H. Wang, X. Liu, B. Li, Y. Li, W. Yu, X. Wang, H. Sun and B. Yang, *Adv. Funct. Mater.*, 2012, **22**, 4732-4740.
- 30 P. Anilkumar, X. Wang, L. Cao, S. Sahu, J. H. Liu, P. Wang, K. Korch, K. N. Tackett, A. Parenzan and Y.-P. Sun, *Nanoscale*, 2011, **3**, 2023-2027.
- 31 Y.-P. Sun, X. Wang, F. Lu, L. Cao, M. J. Meziani, P. G. Luo, L. Gu and L. M. Veca, *J. Phys. Chem. C*, 2008, **112**, 18295-18298.
- 32 Y. Dong, H. Pang, H. B. Yang, C. Guo, J. Shao, Y. Chi, C. M. Li and T. Yu, *Angew. Chem. Int. Ed.*, 2013, **52**, 7800-7804.
- 33 L. Liu, Y. Li, L. Zhan, Y. Liu and C. Huang, *Sci. China. Chem.*, 2011, **54**, 1342-1347.
- 34 X. Yang, Y. Zhuo, S. Zhu, Y. Luo, Y. Feng and Y. Dou, *Biosens. Bioelectron.*, 2014, **60**, 292-298.
- 35 X. Li, S. Zhu, B. Xu, K. Ma, J. Zhang, B. Yang and W. Tian, *Nanoscale*, 2013, **5**, 7776-7779.
- 36 Y. Guo, Z. Wang, H. Shao and X. Jiang, *Carbon*, 2013, **52**, 583-589.
- 37 M. J. Krysmann, A. Kelarakis, P. Dallas and E. P. Giannelis, *J. Am. Chem. Soc.*, 2012, **134**, 747-750.
- 38 S. Zhu, Q. Meng, L. Wang, J. Zhang, Y. Song, H. Jin, K. Zhang, H. Sun, H. Wang and B. Yang, *Angew. Chem. Int. Ed.*, 2013, **52**, 3953-3957.
- 39 X. Teng, C. Ma, C. Ge, M. Yan, J. Yang, Y. Zhang, P. C. Morais and H. Bi, *J. Mater. Chem. B*, 2014, **2**, 4631-4639.
- 40 A. Zhao, C. Zhao, M. Li, J. Ren and X. Qu, *Anal. Chim. Acta*, 2014, **809**, 128-133.
- 41 H. Zhang, Y. Chen, M. Liang, L. Xu, S. Qi, H. Chen and X. Chen, *Anal. Chem.*, 2014, **86**, 9846-9852.
- 42 Z. Qian, J. Ma, X. Shan, H. Feng, L. Shao and J. Chen, *Chemistry*, 2014, **20**, 2254-2263.
- 43 X. Ran, H. Sun, F. Pu, J. Ren and X. Qu, *Chem. Commun.*, 2013, **49**, 1079-1081.
- 44 R. Liu, H. Li, W. Kong, J. Liu, Y. Liu, C. Tong, X. Zhang and Z. Kang, *Mater. Res. Bull.*, 2013, **48**, 2529-2534.
- 45 Y. Liu, C.-Y. Liu and Z.-Y. Zhang, *Appl. Surface. Sci.*, 2012, **263**, 481-485.
- 46 Y. Zhai, Z. Zhu, C. Zhu, J. Ren, E. Wang and S. Dong, *J. Mater. Chem. B*, 2014, **2**, 6995-6999.
- 47 K. Qu, J. Wang, J. Ren and X. Qu, *Chem. Eur. J.*, 2013, **19**, 7243-7249.
- 48 Y. Song, S. Zhu, S. Xiang, X. Zhao, J. Zhang, H. Zhang, Y. Fu and B. Yang, *Nanoscale*, 2014, **6**, 4676-4682.
- 49 S. Hu, Q. Zhao, Q. Chang, J. Yang and J. Liu, *RSC Adv.*, 2014, **4**, 41069-41075.
- 50 F. Yan, Y. Zou, M. Wang, X. Mu, N. Yang and L. Chen, *Sens. Actuators B*, 2014, **192**, 488-495.
- 51 Y. Xu, C.-J. Tang, H. Huang, C.-Q. Sun, Y.-K. Zhang, Q.-F. Ye and A.-J. Wang, *Chinese. J. Anal. Chem.*, 2014, **42**, 1252-1258.
- 52 R. Zhang and W. Chen, *Biosens. Bioelectron.*, 2014, **55**, 83-90.
- 53 W. Wang, T. Kim, Z. Yan, G. Zhu, I. Cole, N. T. Nguyen and Q. Li, *J. Colloid. Interface. Sci.*, 2015, **437**, 28-34.
- 54 J. Wei, X. Zhang, Y. Sheng, J. Shen, P. Huang, S. Guo, J. Pan and B. Feng, *Mater. Lett.*, 2014, **123**, 107-111.
- 55 H. X. Zhao, L. Q. Liu, Z. D. Liu, Y. Wang, X. J. Zhao and C. Z. Huang, *Chem. Commun.*, 2011, **47**, 2604-2606.
- 56 J. M. Bai, L. Zhang, R. P. Liang and J. D. Qiu, *Chem. Eur. J.*, 2013, **19**, 3822-3826.
- 57 J. J. Liu, X. L. Zhang, Z. X. Cong, Z. T. Chen, H. H. Yang and G. N. Chen, *Nanoscale*, 2013, **5**, 1810-1815.
- 58 J. Xu, Y. Zhou, G. Cheng, M. Dong, S. Liu, *Luminescence*, 2014, **30**, 411-415.
- 59 S. Zhang, Q. Wang, G. Tian and H. Ge, *Mater. Lett.*, 2014, **115**, 233-236.
- 60 X. Zhu, H. Wang, Q. Jiao, X. Xiao, X. Zuo, Y. Liang, J. Nan, J. Wang and L. Wang, *Part. Part. Syst. Char.*, 2014, **31**, 771-777.
- 61 Z. Jiang, A. Nolan, J. G. Walton, A. Lilienkampff, R. Zhang and M. Bradley, *Chem. Eur. J.*, 2014, **20**, 10926-10931.
- 62 X. Wang, K. Qu, B. Xu, J. Ren and X. Qu, *J. Mater. Chem.*, 2011, **21**, 2445.
- 63 S. S. Wee, Y. H. Ng and S. M. Ng, *Talanta*, 2013, **116**, 71-76.
- 64 D. Pan, J. Zhang, Z. Li and M. Wu, *Adv. Mater.*, 2010, **22**, 734-738.
- 65 D. Pan, L. Guo, J. Zhang, C. Xi, Q. Xue, H. Huang, J. Li, Z. Zhang, W. Yu, Z. Chen, Z. Li and M. Wu, *J. Mater. Chem.*, 2012, **22**, 3314.
- 66 D. Pan, J. Zhang, Z. Li, C. Wu, X. Yan and M. Wu, *Chem. Commun.*, 2010, **46**, 3681-3683.
- 67 J. Peng, W. Gao, B. K. Gupta, Z. Liu, R. Romero-Aburto, L. Ge, L. Song, L. B. Alemany, X. Zhan, G. Gao, S. A. Vithayathil, B. A. Kaiparettu, A. A. Marti, T. Hayashi, J. J. Zhu and P. M. Ajayan, *Nano Lett.*, 2012, **12**, 844-849.
- 68 F. Yang, M. Zhao, B. Zheng, D. Xiao, L. Wu and Y. Guo, *J. Mater. Chem.*, 2012, **22**, 25471.
- 69 Y. Hu, J. Yang, J. Tian, L. Jia and J. Yu, *Carbon*, 2014, **77**, 775-782.
- 70 Y. Dong, N. Zhou, X. Lin, J. Lin, Y. Chi and G. Chen, *Chem. Mater.*, 2010, **22**, 5895-5899.
- 71 Y. Dong, C. Chen, X. Zheng, L. Gao, Z. Cui, H. Yang, C. Guo, Y. Chi and C. M. Li, *J. Mater. Chem.*, 2012, **22**, 8764.
- 72 M. Wu, Y. Wang, W. Wu, C. Hu, X. Wang, J. Zheng, Z. Li, B. Jiang and J. Qiu, *Carbon*, 2014, **78**, 480-489.
- 73 Q. L. Zhao, Z. L. Zhang, B. H. Huang, J. Peng, M. Zhang and D. W. Pang, *Chem. Commun.*, 2008, **41**, 5116-5118.
- 74 R.-J. Fan, Q. Sun, L. Zhang, Y. Zhang and A.-H. Lu, *Carbon*, 2014, **71**, 87-93.
- 75 C.-F. W. J. Wang and S. Chen, *Angew. Chem. Int. Ed.*, 2012, **51**, 9297-9301.
- 76 D. Sun, R. Ban, P.-H. Zhang, G.-H. Wu, J.-R. Zhang and J.-J. Zhu, *Carbon*, 2013, **64**, 424-434.
- 77 C. Jiang, H. Wu, X. Song, X. Ma, J. Wang and M. Tan, *Talanta*, 2014, **127**, 68-74.
- 78 S. Gomez-de Pedro, A. Salinas-Castillo, M. Ariza-Avidad, A. Lapresta-Fernandez, C. Sanchez-Gonzalez, C. S. Martinez-

- Cisneros, M. Puyol, L. F. Capitan-Vallvey and J. Alonso-Chamarro, *Nanoscale*, 2014, **6**, 6018-6024.
- 79 H. Nie, M. Li, Q. Li, S. Liang, Y. Tan, L. Sheng, W. Shi and S. X.-A. Zhang, *Chem. Mater.*, 2014, **26**, 3104-3112.
- 80 Y. Dong, J. Shao, C. Chen, H. Li, R. Wang, Y. Chi, X. Lin and G. Chen, *Carbon*, 2012, **50**, 4738-4743.
- 81 Y. Dong, G. Li, N. Zhou, R. Wang, Y. Chi and G. Chen, *Anal. Chem.*, 2012, **84**, 8378-8382.
- 82 Z. Huang, F. Lin, M. Hu, C. Li, T. Xu, C. Chen and X. Guo, *J. Lumin.*, 2014, **151**, 100-105.
- 83 Y. Dong, R. Wang, H. Li, J. Shao, Y. Chi, X. Lin and G. Chen, *Carbon*, 2012, **50**, 2810-2815.
- 84 Y. Dong, R. Wang, G. Li, C. Chen, Y. Chi and G. Chen, *Anal. Chem.*, 2012, **84**, 6220-6224.
- 85 A. Salinas-Castillo, M. Ariza-Avidad, C. Pritz, M. Camprubi-Robles, B. Fernandez, M. J. Ruedas-Rama, A. Megia-Fernandez, A. Lapresta-Fernandez, F. Santoyo-Gonzalez, A. Schrott-Fischer and L. F. Capitan-Vallvey, *Chem. Commun.*, 2013, **49**, 1103-1105.
- 86 H. Sun, N. Gao, L. Wu, J. Ren, W. Wei and X. Qu, *Chem. Eur. J.*, 2013, **19**, 13362-13368.
- 87 Q. Qu, A. Zhu, X. Shao, G. Shi and Y. Tian, *Chem. Commun.*, 2012, **48**, 5473-5475.
- 88 X. Liu, N. Zhang, T. Bing and D. Shangguan, *Anal. Chem.*, 2014, **86**, 2289-2296.
- 89 X. Lin, G. Gao, L. Zheng, Y. Chi and G. Chen, *Anal. Chem.*, 2014, **86**, 1223-1228.
- 90 A. Zhu, Q. Qu, X. Shao, B. Kong and Y. Tian, *Angew. Chem. Int. Ed.*, 2012, **51**, 7185-7189.
- 91 Y. Dong, R. Wang, W. Tian, Y. Chi and G. Chen, *RSC Adv.*, 2014, **4**, 3701.
- 92 H. Gonçalves, P. A. S. Jorge, J. R. A. Fernandes and J. C. G. Esteves da Silva, *Sens. Actuators, B*, 2010, **145**, 702-707.
- 93 H. M. Gonçalves, A. J. Duarte and J. C. Esteves da Silva, *Biosens. Bioelectron.*, 2010, **26**, 1302-1306.
- 94 Y. H. Li, L. Zhang, J. Huang, R. P. Liang and J. D. Qiu, *Chem. Commun.*, 2013, **49**, 5180-5182.
- 95 Z. Qu, X. Zhou, L. Gu, R. Lan, D. Sun, D. Yu and G. Shi, *Chem. Commun.*, 2013, **49**, 9830-9832.
- 96 P. Shen and Y. Xia, *Anal. Chem.*, 2014, **86**, 5323-5329.
- 97 Y. Shi, Y. Pan, H. Zhang, Z. Zhang, M. J. Li, C. Yi and M. Yang, *Biosens. Bioelectron.*, 2014, **56**, 39-45.
- 98 H. Dai, Y. Shi, Y. Wang, Y. Sun, J. Hu, P. Ni and Z. Li, *Sens. Actuators, B*, 2014, **202**, 201-208.
- 99 W. Wei, C. Xu, J. Ren, B. Xu and X. Qu, *Chem. Commun.*, 2012, **48**, 1284-1286.
- 100 Z. S. Qian, X. Y. Shan, L. J. Chai, J. J. Ma, J. R. Chen and H. Feng, *Nanoscale*, 2014, **6**, 5671-5674.
- 101 Z. S. Qian, X. Y. Shan, L. J. Chai, J. J. Ma, J. R. Chen and H. Feng, *Biosens. Bioelectron.*, 2014, **60**, 64-70.
- 102 H. Li, J. Zhai, J. Tian, Y. Luo and X. Sun, *Biosens. Bioelectron.*, 2011, **26**, 4656-4660.
- 103 X. Cui, L. Zhu, J. Wu, Y. Hou, P. Wang, Z. Wang and M. Yang, *Biosens. Bioelectron.*, 2015, **63**, 506-512.
- 104 L. Zhu, X. Cui, J. Wu, Z. Wang, P. Wang, Y. Hou and M. Yang, *Anal. Methods*, 2014, **6**, 4430-4436.
- 105 H. Zhao, Y. Chang, M. Liu, S. Gao, H. Yu and X. Quan, *Chem. Commun.*, 2013, **49**, 234-236.
- 106 D. Bu, H. Zhuang, G. Yang and X. Ping, *Sens. Actuators, B*, 2014, **195**, 540-548.
- 107 Y. Wang, L. Zhang, R. P. Liang, J. M. Bai and J. D. Qiu, *Anal. Chem.*, 2013, **85**, 9148-9155.
- 108 A. Cayuela, M. L. Soriano and M. Valcarcel, *Ana. Chim. Acta*, 2013, **804**, 246-251.
- 109 I. Costas-Mora, V. Romero, I. Lavilla and C. Bendicho, *Anal. Chem.*, 2014, **86**, 4536-4543.
- 110 S. Li, J. Luo, G. Yin, Z. Xu, Y. Le, X. Wu, N. Wu and Q. Zhang, *Sens. Actuators, B*, 2015, **206**, 14-21.
- 111 W. Miao, *Chem. Rev.*, 2008, **108**, 2506-2553.
- 112 L. Zheng, Y. Chi, Y. Dong, J. Lin and B. Wang, *J. Am. Chem. Soc.*, 2009, **131**, 4564-4565.
- 113 L. Li, J. Ji, R. Fei, C. Wang, Q. Lu, J. Zhang, L. Jiang and J. Zhu, *Adv. Funct. Mater.*, 2012, **22**, 2971-2979.
- 114 Y. Chen, Y. Dong, H. Wu, C. Chen, Y. Chi and G. Chen, *Electrochim. Acta*, 2015, **151**, 552-557.
- 115 Q. Lu, W. Wei, Z. Zhou, Z. Zhou, Y. Zhang and S. Liu, *Analyst*, 2014, **139**, 2404-2410.
- 116 S. Yang, J. Liang, S. Luo, C. Liu and Y. Tang, *Anal. Chem.*, 2013, **85**, 7720-7725.
- 117 T. T. Zhang, H. M. Zhao, X. F. Fan, S. Chen and X. Quan, *Talanta*, 2015, **131**, 379-385.
- 118 L. Wu, M. Li, M. Zhang, M. Yan, S. Ge and J. Yu, *Sens. Actuators, B*, 2013, **186**, 761-767.
- 119 M. Su, H. Liu, L. Ge, Y. Wang, S. Ge, J. Yu and M. Yan, *Electrochim. Acta*, 2014, **146**, 262-269.
- 120 M. Zhang, H. Liu, L. Chen, M. Yan, L. Ge, S. Ge and J. Yu, *Biosens. Bioelectron.*, 2013, **49**, 79-85.
- 121 J. Lou, S. Liu, W. Tu and Z. Dai, *Anal. Chem.*, 2015, **87**, 1145-1151.
- 122 Y. Dong, C. Chen, J. Lin, N. Zhou, Y. Chi and G. Chen, *Carbon*, 2013, **56**, 12-17.
- 123 Y. Dong, W. Tian, S. Ren, R. Dai, Y. Chi and G. Chen, *ACS Appl. Mater. Interfaces*, 2014, **6**, 1646-1651.
- 124 J. Lu, M. Yan, L. Ge, S. Ge, S. Wang, J. Yan and J. Yu, *Biosens. Bioelectron.*, 2013, **47**, 271-277.
- 125 Y. Dong, R. Dai, T. Dong, Y. Chi and G. Chen, *Nanoscale*, 2014, **6**, 11240-11245.
- 126 M. Zhang, L. Bai, W. Shang, W. Xie, H. Ma, Y. Fu, D. Fang, H. Sun, L. Fan, M. Han, C. Liu and S. Yang, *J. Mater. Chem.*, 2012, **22**, 7461.
- 127 Z. Lin, W. Xue, H. Chen and J. M. Lin, *Chem. Commun.*, 2012, **48**, 1051-1053.
- 128 M. Amjadi, J. L. Manzoori, T. Hallaj and M. H. Sorouraddin, *Spectrochim. Acta. A*, 2014, **122**, 715-720.
- 129 Z. Lin, W. Xue, H. Chen and J. M. Lin, *Anal. Chem.*, 2011, **83**, 8245-8251.
- 130 W. Xue, Z. Lin, H. Chen, C. Lu and J. M. Lin, *J. Phys. Chem. C*, 2011, **115**, 21707-21714.
- 131 J. Shi, C. Lu, D. Yan and L. Ma, *Biosens. Bioelectron.*, 2013, **45**, 58-64.
- 132 M. Amjadi, J. L. Manzoori and T. Hallaj, *J. Lumin.*, 2014, **153**, 73-78.